iScience

CellPress
OPEN ACCESS

Article

The "weaken-fill-repair" model for cell budding: Linking cell wall biosynthesis with mechanics

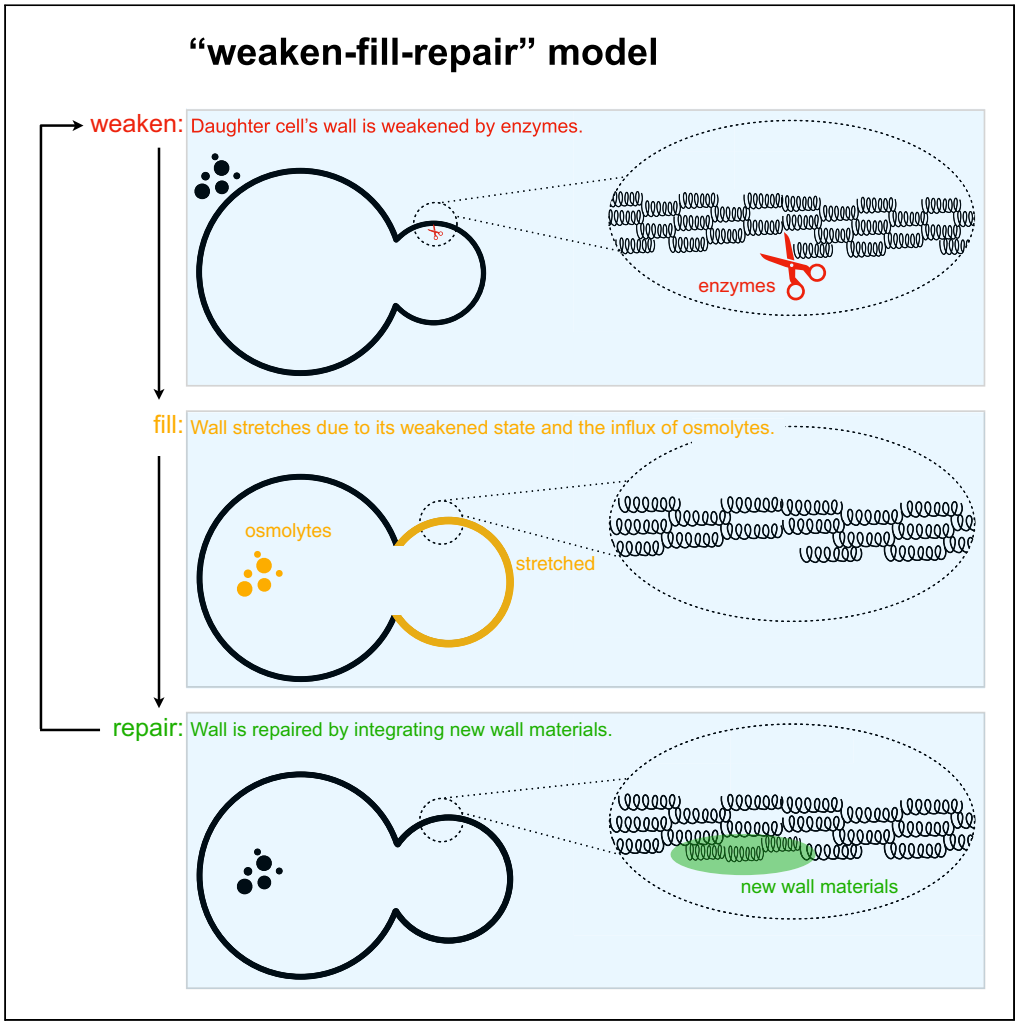

Yu Liu, Chunxiuzi Liu, Shaohua Tang, ..., Zengru Di, Da Zhou, Matthias Heinemann

yu.ernest.liu@bnu.edu.cn

Highlights

Proposes a quantitative weaken-fill-repair model for yeast cell budding

Predicts often-overlooked oscillatory size changes in mother cells during budding

Pinpoints a single critical parameter that governs the entire budding process

Suggests homeostasis is achieved only through asymmetric division, for cell budding

Liu et al., iScience 27, 110981
October 18, 2024
https://doi.org/10.1016/j.isci.2024.110981

iScience

CellPress
OPEN ACCESS

Article

The "weaken-fill-repair" model for cell budding: Linking cell wall biosynthesis with mechanics

Yu Liu,[1,2,7,8,*] Chunxiuzi Liu,[1,2,3,7] Shaohua Tang,[1,2,3,4] Hui Xiao,[1,2] Xinlin Wu,[1,2] Yunru Peng,[1,2] Xianyi Wang,[1,2] Linjie Que,[1,2] Zengru Di,[1,2] Da Zhou,[5] and Matthias Heinemann[6]

SUMMARY

The interplay between cellular mechanics and biochemical processes in the cell cycle is not well understood. We propose a quantitative model of cell budding in *Saccharomyces cerevisiae* as a "weaken-fill-repair" process, linking Newtonian mechanics of the cell wall with biochemical changes that affect its properties. Our model reveals that (1) oscillations in mother cell size during budding are an inevitable outcome of the process; (2) asymmetric division is necessary for the daughter cell to maintain mechanical stiffness; and (3) although various aspects of the cell are constrained and interconnected, the budding process is governed by a single reduced parameter, ψ, which balances osmolyte accumulation with enzymatic wall-weakening to ensure homeostasis. This model provides insights into the evolution of cell walls and their role in cell division, offering a system-level perspective on cell morphology.

INTRODUCTION

Cell growth and division involve an intricate genetic and metabolic network that controls the timely execution of the bioprocesses involved in the start and completion of the cell cycle.[1–4] Despite the intricacy of this network, the highest-level determinants of morphological changes related to cell cycle progression are the laws of physics. Specifically, it is the Newtonian mechanics of the cell's boundary that ultimately governs any changes in cellular size and shape, allowing for cell expansion and, eventually, cell division.[5–7] However, how the interplay between mechanics and other cellular processes influences the manifestation of the cell cycle is poorly understood.[8]

In cells with cell wall, the wall imposes a major physical constraint for morphogenesis. Morphogenetic events induce deformations of the cell wall,[9,10] which in turn depend on cell wall expansion,[11] turgor pressure,[12–14] and the mechanical properties of the cell wall.[15,16] There is empirical evidence that on time scales in the order of minutes, the cell wall behaves as an elastic material, like a spring network[13,17,18]; while on longer time scales (e.g., hours), the wall behaves as a plastic material or viscous fluid (like a pitch), that is, if any deformation of the cell wall (caused e.g., by the stress exerted by osmotic pressure) exceeds a certain threshold, this deformation is then irreversible.[10,19] Although the deformation threshold is difficult to determine and often takes an arbitrary value in models, the growth and expansion of the cell are thought to be the results of this irreversible deformation.[20,21] Understanding how the interplay between these factors defines cell cycle-related morphogenetic events is challenging.[22–24]

Here, we developed a quantitative, dynamic model—which could be summarized as an iterative "weaken-fill-repair" process—based on variables including the geometrical parameters, the mechanical properties of the cell and the dynamics of osmotic pressure, particularly for budding yeast *Saccharomyces cerevisiae* whose process of cell division is characterized by morphogenetic asymmetry.[6,25,26] This model describes how the Newtonian mechanics over the cell wall, coupled with the biochemical processes that change the mechanical properties of the wall, exert control over the budding process. By relying solely on those variables, our model predicts an unexpected, yet experimentally observed, size oscillation of the mother cell compartment during budding, and demonstrates the interplay of these variables as key morphogenetic factors. Furthermore, our model suggests that Newtonian mechanics play a significant role in determining the asymmetry of yeast cell division, and this asymmetry enables the newborn daughter cell to maintain mechanical stiffness similar to that of its mother. Our model serves as a quantitative tool to investigate morphogenesis from a systemic perspective, offering insights that could be utilized both for characterizing developmental events[27,28] and for investigations of cell size control.

[1]Department of Systems Science, Faculty of Arts and Sciences, Beijing Normal University, Zhuhai, China
[2]International Academic Center of Complex Systems, Beijing Normal University, Zhuhai, China
[3]School of Systems Science, Beijing Normal University, Beijing, China
[4]Center for Cognition and Neuroergonomics, State Key Laboratory of Cognitive Neuroscience and Learning, Beijing Normal University, Zhuhai, China
[5]School of Mathematical Sciences, Xiamen University, Xiamen, China
[6]Molecular Systems Biology, Groningen Biomolecular Sciences and Biotechnology Institute, University of Groningen, 9747AG Groningen, The Netherlands
[7]These authors contributed equally
[8]Lead contact
*Correspondence: yu.ernest.liu@bnu.edu.cn
https://doi.org/10.1016/j.isci.2024.110981

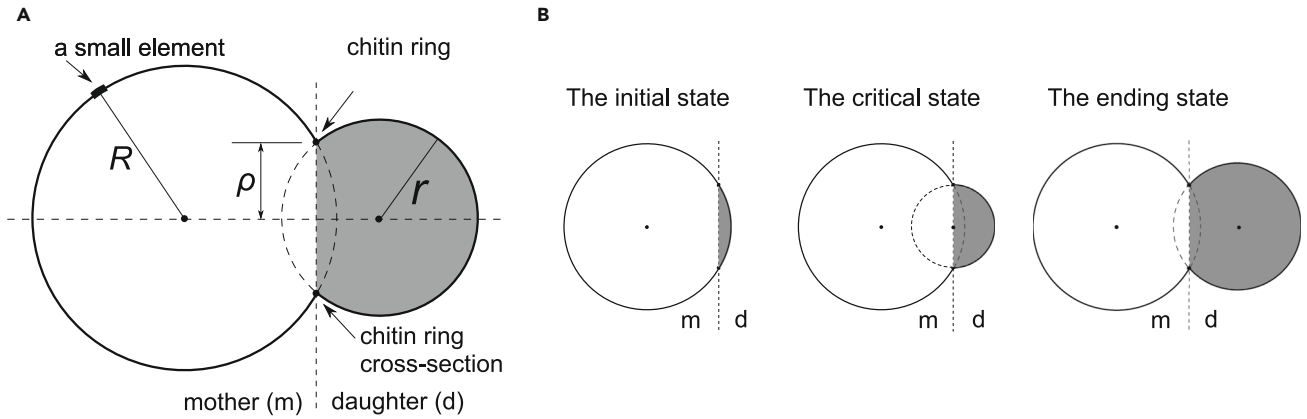

Figure 1. Representation of the cell in the model

(A) Sketch of the whole cell. Note that each part of the cell is not a complete sphere; thus, for example, when calculating the volume of the mother, we only consider the volume of the white part.

(B) Three distinct states during the budding process.

Model

The geometry of the cell

To construct a quantitative biophysical model of the budding process, we assumed that the whole yeast cell consists of two partial spheres (Figure 1A). We call the part on the left-hand side of the vertical dash line the mother and the right-hand side the daughter. The overlapping region of these two incomplete spheres is a circle, whose radius is denoted as ρ, corresponding to the chitin ring formed during yeast cell budding, which is rigid and stays almost unchanged during the whole budding process.[6,17] We assume that the mother can be approximated by a sphere, and thus, any element on the mother's surface has the same radius of curvature, denoted as *R*, which is equal to the radius of the projected sphere. The radius of curvature of the daughter *r* is defined in the same way.

During budding, the shape of the cell changes. We can define three different time points corresponding to three states of the cell (Figure 1B). The first is the initial state when the cell is about to deform. At this initial state, the rigid chitin ring has been formed, and both the daughter and the mother have the same radius of curvature. Note that even though the cell has not deformed yet, we still call the gray part in Figure 1B as the daughter. The second state is the critical state when the daughter has grown to the extent that its radius of curvature, *r*, equals the chitin ring's radius. We call it the critical state because, before this state, *r* decreases as the daughter grows, while after this state, *r* increases as the daughter grows (that is, after the critical state, *r* is always equal to the radius of the daughter, from which the size indicators such as volume and circumference can be calculated). The last state is the ending state. It is when cytokinesis occurs and the daughter detaches from the mother.

Empirical-data-based assumptions

Based on the aforementioned cellular geometry, we develop a quantitative model of the cell wall expansion and budding process, using the following assumptions, which are based on empirical observations:

1. The whole budding process is quasi-static, which means that, most of the time, the entire cell wall surface is in mechanical equilibrium, i.e., the net force exerted on any small element of the cell wall is zero.[29–31].
2. Every now and then, the mechanical equilibrium is temporarily broken by (1) a slight weakening of the daughter's cell wall at the budding position due to enzymatic activity[6,32] and (2) the accumulation of osmolytes inside the cell.[8,22,33] Such temporarily broken equilibrium is rapidly replaced by a new mechanical equilibrium achieved by a slight adjustment of the mother's and daughter's radius, which results in a slight expansion of the cell. We call this the "weaken-fill" process.
3. Then, new cell wall materials are integrated into the weakened wall of the daughter to relieve its increased strain and restore its strength.[34–36] We call this the "repair" process.

This whole "weaken-fill-repair" process repeats, resulting in the bud's growth, and the derivation and simulation of this process will be discussed later. In fact, there exists experimental evidence indirectly supporting the ongoing weakening processes of the cell wall, and the concept that the growing cell wall must be "weakened" to expand its surface is derived from various biophysical, biochemical, and physiological considerations.[37,38] Refer to STAR Methods - method details for additional empirical evidence supporting our assumptions, and for the differences between our model and the classic model of cell growth, the pump-leak mechanism (PLM).[39,40] Our model does not explicitly include the interactions between gene regulations and cell growth[41–44]; Instead, it considers that the effects of these factors ensure that the cell wall meets quasi-static conditions during the budding process. Our model also differs from phenomenological models,[45,46] as our

emphasis is on the mechanism from a mechanical perspective, enabling us to develop the model by integrating the process over time from scratch.

Mechanical equations for the cell

Now, we derive the mechanical equations that govern the cell's state. At any stage during the whole budding process, for any small element on the wall surface (Figure 1A), Newton's second law governs its spatial movement. Choosing the direction away from the center of the sphere as the positive direction, the Newtonian equation can be written as:

$$\Pi \cdot \pi R^2 - \sigma h \cdot 2\pi R = M \cdot a \quad \text{(Equation 1)}$$

where Π [N/m^2] is the difference of osmotic pressure inside and outside the cell,[47] σ [N/m^2] is the mechanical stress exerted by this element (namely, the intensity of the internal force that arises within the element as a reaction to external forces applied to it), h [m] is the element's thickness, M [kg] is its mass, and a [m/s^2] is its acceleration. The first term comes from the osmotic pressure difference, which results in a mechanical force pushing this element outwards; while the second term comes from the stress exerted by this wall element's neighboring elements, which results in a mechanical force dragging this element inwards.

Based on the Van't Hoff equation, which is a quantitative relationship between osmotic pressure and solute concentration, the difference of osmotic pressure inside and outside the cell can be written as[48]:

$$\Pi = \lambda \cdot (N/V - c_{ex}) \equiv \lambda \cdot C(N, R, r) \quad \text{(Equation 2)}$$

where λ [J/mol] is a constant, equal to the product of the Van't Hoff index of osmolytes, the gas constant, and the temperature, N [mol] is the total osmolyte amount inside the cell, c_{ex} [mol/m^3] is the osmolyte concentration outside the cell, and V [m^3] is the cell's total volume, a function of R and r (note that V is also a function of the rigid chitin ring radius ρ, as illustrated in Figure 1; but since ρ remains constant during the budding process, it is incorporated as a fixed parameter in the calculation of V). For convenience, we write the term $(N/V - c_{ex})$ (namely the difference of osmolyte concentration inside and outside the cell) as C [mol/m^3], a function of N, R and r, with treating c_{ex} as a constant.

Now, we can derive the Newtonian equations for the mother. By employing Equation 2, we can rewrite Equation 1 specifically for an element from the mother cell:

$$(\lambda C \cdot R/2 - \sigma_m h_m) \cdot R = M_m a_m / (2\pi) \quad \text{(Equation 3)}$$

where the subscript m represents the quantities from the mother. We further assume that the wall materials of the mother are incompressible,[18,49] so the volume of the wall stays constant:

$$S_{m0} \cdot h_{m0} = S_m(R) \cdot h_m(R) \quad \text{(Equation 4)}$$

where S_m is the surface area of the mother. Note that S_m and h_m are functions of R, and the subscript "0" represents quantities at the initial state (Figure 1B).

Moreover, we assume that the wall materials of the mother are linear-elastic and isotropic,[18] so we can employ Lagrangian strain and apply Hooke's law to this element[47]:

$$\epsilon_m(R) = L_m(R)/l_m - 1 \quad \text{(Equation 5)}$$

$$\sigma_m = k_m \cdot \epsilon_m(R) \quad \text{(Equation 6)}$$

where ϵ_m is the Lagrangian strain (a dimensionless quantity) of mother's cell wall, describing its deformation compared to the original shape; and k_m [N/m^2] is a constant which represents the stiffness of the mother's cell wall (corresponding to Young's modulus). The ratio L_m/l_m represents the circumferential extension, where L_m is the stretched circumference of the mother's wall (namely the circumference of the white part in Figure 1A), and l_m is the unstretched circumference, i.e., l_m is the circumference of the mother's wall when the osmotic pressure inside and outside the cell are identical. We further assume that the mechanical properties of the mother's wall are constant, i.e., k_m and l_m stay constant.

Because of the quasi-static assumption as mentioned, at the initial state, any element on the cell wall is in mechanical equilibrium, meaning that the net force exerted on each element is zero, and thus the acceleration is zero. So, at the initial state, we have

$$\lambda C_0 \cdot R_0/2 - k_m \epsilon_{m0} h_{m0} = 0 \quad \text{(Equation 7)}$$

By incorporating Equation 4 - Equation 7 into Equation 3, we have the overall Equation 8 for Newtonian mechanics of the mother:

$$\left(\frac{C}{C_0}\frac{R}{R_0} - \frac{\epsilon_m}{\epsilon_{m0}}\frac{1}{S_m/S_{m0}}\right) \cdot \frac{R}{R_0} = \frac{a_m}{\pi \lambda C_0 R_0^2/M_m} \quad \text{(Equation 8)}$$

Following the same logic, we can derive an equation to describe the mechanics of the daughter (see STAR Methods - method details).

From this point on, we will normalize the equations for both the mother and daughter cells, to facilitate more convenient analysis in subsequent steps. Using normalized quantities instead of quantities with physical units has several advantages. Most importantly, all quantities

Table 1. Normalization for all quantities

Mother's radius of curvature	$\tilde{R} = R/R_0$
Daughter's radius of curvature	$\tilde{r} = r/R_0$
Chitin ring radius	$\tilde{\rho} = \rho/R_0$
Osmolyte amount inside the cell	$\tilde{N} = N/N_0$
Total volume of the cell	$\tilde{V}(\tilde{R},\tilde{r}) = V(R,r)/V_0$
External osmolyte concentration	$\tilde{c}_{ex} = c_{ex}/(N_0/V_0)$
Osmolyte concentration difference	$\tilde{C}(\tilde{N},\tilde{R},\tilde{r}) = C(N,R,r)/C_0$
Surface area of mother	$\tilde{S}_m(\tilde{R}) = S_m(R)/S_{m0}$
Circumference of mother	$\tilde{L}_m(\tilde{R}) = L_m(R)/R_0$
Circumference of daughter	$\tilde{L}_d(\tilde{r}) = L_d(r)/R_0$
Unstretched circumference of mother	$\tilde{l}_m = l_m/R_0$
Unstretched circumference of daughter	$\tilde{l}_d = l_d/R_0$
Lagrangian strain of mother	$\tilde{\epsilon}_m(\tilde{R}) = \epsilon_m(R)/\epsilon_{m0}$
Lagrangian strain of daughter	$\tilde{\epsilon}_d(\tilde{r},\tilde{l}_d) = \epsilon_d(r,l_d)/\epsilon_{m0}$
Acceleration of mother's element	$\tilde{a}_m = a_m/a_{m0}$
Acceleration of daughter's element	$\tilde{a}_d = a_d/a_{d0}$
Surface modulus of daughter	$\tilde{\eta} = \eta/\eta_0$
Unstretched volume of the cell	$\tilde{V}_u = V_u/V_0$
Osmotic pressure difference	$\tilde{\Pi} = \Pi/(\lambda C_0)$

are then relative, which is often more robust than measurements in absolute units. Secondly, the number of parameters in equations can be largely reduced. Last but not least, biological quantities in one equation can differ by many orders of magnitude, which makes the numerical solution of the equation very unstable. This means that a small error in the parameters of the equation will lead to very different solutions. Writing equations in the normalized form naturally solves this problem. See STAR Methods - method details for the normalization details, and see Table 1 for what these quantities stand for. Equation 8 is normalized as Equation 9, the Newtonian equation of the mother, while Equation 23 (in STAR Methods - method details) is normalized as Equation 10, the Newtonian equation of the daughter:

$$\left[\tilde{C}(\tilde{N},\tilde{R},\tilde{r})\cdot\tilde{R}-\frac{\tilde{\epsilon}_m(\tilde{R})}{\tilde{S}_m(\tilde{R})}\right]\cdot\tilde{R}=\tilde{a}_m \qquad \text{(Equation 9)}$$

$$[\tilde{C}(\tilde{N},\tilde{R},\tilde{r})\cdot\tilde{r}-\tilde{\eta}\cdot\tilde{\epsilon}_d(\tilde{r},\tilde{l}_d)]\cdot\tilde{r}=\tilde{a}_d \qquad \text{(Equation 10)}$$

where $\tilde{\eta}$ is the surface modulus of the daughter, representing the stiffness or "strength" of the daughter's wall, and $\tilde{l}_d$ is the unstretched circumference of the daughter (both are normalized quantities). Notice that a quantity with a superscript tilde ~ above always represents a normalized quantity. Finally, it is important to note that the formulas describing the mother and the daughter (Equations 9 and 10) are different. This is because we assumed that the mother's cell wall is incompressible (Equation 4), whereas the daughter's cell wall changes properties during budding.

Specifically, more wall materials will be integrated into the daughter during budding (see STAR Methods - method details). As a result, the daughter's cell wall does not have the same constraint as the mother that can be expressed in the form of Equation 9. Therefore, we simply encompass the mechanical properties of the daughter's cell wall into a variable $\tilde{\eta}$, the surface modulus, which represents the stiffness or "strength" of the wall.

Mechanical equilibrium and dynamics

Until now, we merely described the state of the cell, with the dynamics missing. Now, we will incorporate the dynamics into the model. To do so, we will make several assumptions, and then couple the Newtonian equations of the mother and the daughter, to finally give a quantitative description of the whole budding process.

The first assumption is that most of the time during the budding process, each element on the cell wall surface is in mechanical equilibrium, that is, the net force exerted on each element is zero, and the acceleration is thus zero (note that this is the quasi-static assumption, and the mechanical equilibrium will be broken now and then to allow for wall expansion, as we shall see later). Therefore, the right-hand side of Equations 9 and 10 are zero, and then we arrive at the two most fundamental equations:

$$\tilde{C}(\tilde{N},\tilde{R},\tilde{r})\cdot\tilde{R}-\tilde{\epsilon}_m(\tilde{R})/\tilde{S}_m(\tilde{R})=0 \qquad \text{(Equation 11)}$$

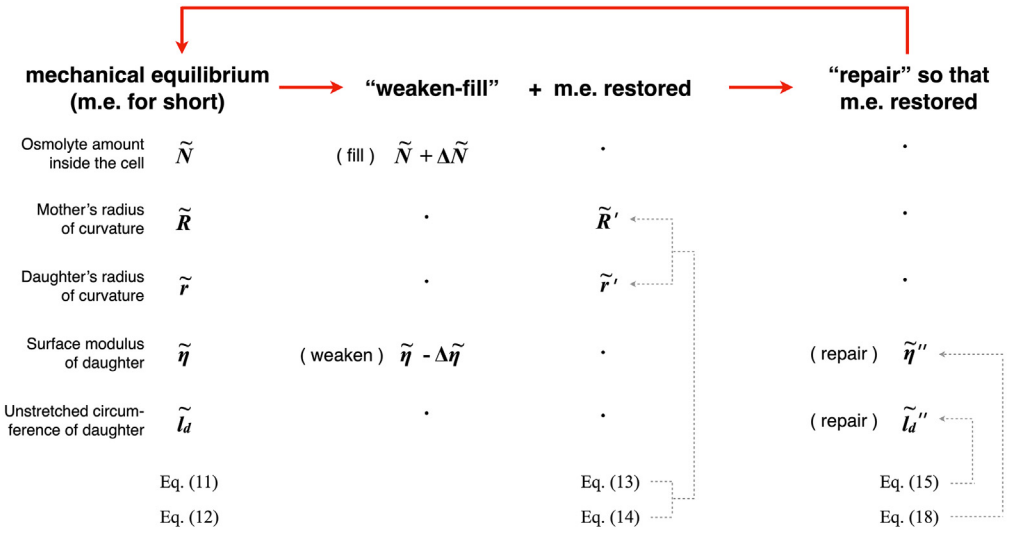

Figure 2. A schematic representation of the budding process in the model

The dots indicate that the corresponding value stays at its previous value. Every complete calculation loop colored in red represents an "iteration step", denoted as *i*.

$$\tilde{C}(\tilde{N},\tilde{R},\tilde{r})\cdot\tilde{r}-\tilde{\eta}\cdot\tilde{\epsilon}_d(\tilde{r},\tilde{l}_d)=0 \qquad \text{(Equation 12)}$$

Another assumption is that the following two infinitesimal processes occur in turn and iteratively, resulting in bud growth (referring to Figure 2 for an overview):

I. "Weaken-fill" process. During this infinitesimal process, the daughter's cell wall is slightly weakened enzymatically (i.e., "weaken") and the osmolyte amount inside the cell is slightly increased (i.e., "fill"). Consequently, the mechanical equilibrium is broken. Then, the radii of the mother and daughter are adjusted immediately so that a new mechanical equilibrium is achieved. Note that, as the daughter's wall is slightly weakened, in order to achieve a new mechanical equilibrium, the daughter's radius will slightly increase and thus be more strained.

II. "Repair" process. After the mere mechanical response at the end of "weaken-fill", a small amount of new wall materials is integrated into the daughter's wall (i.e., "repair"), releasing its strain that increased in the previous process. A new mechanical equilibrium is achieved again. After that, the two processes repeat.

Now, we explain the "weaken-fill" process in more detail. During this process, the daughter's cell wall is slightly weakened, i.e., the surface modulus $\tilde{\eta}$ is changed to $\tilde{\eta}'=\tilde{\eta}-\Delta\tilde{\eta}$ where $\Delta\tilde{\eta}>0$; and the osmolyte amount changes to $\tilde{N}'=\tilde{N}+\Delta\tilde{N}$. We use the prime′ to denote quantities at the end of "weaken-fill". Consequently, the mechanical equilibrium is broken. The radii of the mother and the daughter need to be adjusted immediately to achieve a new equilibrium. So, based on Equations 11 and 12, the following two equilibrium equations have to be satisfied:

$$\tilde{C}(\tilde{N}+\Delta\tilde{N},\tilde{R}',\tilde{r}')\cdot\tilde{R}'-\tilde{\epsilon}_m(\tilde{R}')/\tilde{S}_m(\tilde{R}')=0 \qquad \text{(Equation 13)}$$

$$\tilde{C}(\tilde{N}+\Delta\tilde{N},\tilde{R}',\tilde{r}')\cdot\tilde{r}'-(\tilde{\eta}-\Delta\tilde{\eta})\cdot\tilde{\epsilon}_d(\tilde{r}',\tilde{l}_d)=0 \qquad \text{(Equation 14)}$$

Note that, as can be seen in Equation 14, the weakening process only changes $\tilde{\eta}$ but does not affect its unstretched circumference, i.e., $\tilde{l}_d$ stays unchanged. Now, given $\Delta\tilde{N}$ and $\Delta\tilde{\eta}$, we can solve for the two unknowns $\tilde{R}'$ and $\tilde{r}'$. Therefore, at the end of "weaken-fill", the state of the whole cell becomes $(\tilde{N}+\Delta\tilde{N},\tilde{R}',\tilde{r}',\tilde{\eta}-\Delta\tilde{\eta},\tilde{l}_d)$.

Next, we explain the "repair" process in more detail. After "weaken-fill", the daughter's wall gets weakened and more strained. Here, in the "repair" process, we assume that the increased strain of the daughter will be restored (equivalently, the "strength" of the daughter's wall will be recovered), by integrating new wall materials into the weakened daughter's wall; and we further assume that in "repair", the shape of the whole cell $(\tilde{R}',\tilde{r}')$ and the osmolyte amount $\tilde{N}'$ stay the same as the previous process. In the following, we can derive two equations to calculate the state of the cell at the end of "repair". First, the newly-integrated wall materials will increase the unstretched circumference of the daughter so that the daughter's wall strain is restored to 1, the initial value. So,

$$\tilde{\epsilon}_d(\tilde{r}',\tilde{l}_d'')=1 \qquad \text{(Equation 15)}$$

from which $\tilde{l}''_d$ can be calculated. We use the superscript '' to denote quantities at the end of "repair". Second, as $\tilde{R}'$ and $\tilde{r}'$ do not change in "repair", the two equilibrium equations at the end of "repair" are written as

$$\tilde{C}(\tilde{N}+\Delta\tilde{N},\tilde{R}',\tilde{r}')\cdot\tilde{R}'-\tilde{\epsilon}_m(\tilde{R}')/\tilde{S}_m(\tilde{R}')=0 \quad \text{(Equation 16)}$$

$$\tilde{C}(\tilde{N}+\Delta\tilde{N},\tilde{R}',\tilde{r}')\cdot\tilde{r}'-\tilde{\eta}''\cdot 1=0 \quad \text{(Equation 17)}$$

Note that Equation 16 is exactly the same as Equation 13, and thus satisfied automatically. The first term in Equation 17 is identical to the first term in Equation 14, so in order for Equation 17 to be satisfied, we must have

$$\tilde{\eta}''=(\tilde{\eta}-\Delta\tilde{\eta})\cdot\tilde{\epsilon}_d(\tilde{r}',\tilde{l}_d) \quad \text{(Equation 18)}$$

To conclude, Equations 15 and 18 are the two equations to calculate the state at the end of "repair". It can be interpreted in the following way: Since new wall materials are integrated, not only does the unstretched circumference of the daughter increase from $\tilde{l}_d$ to $\tilde{l}''_d$, but the surface modulus of the daughter's wall also increases from $(\tilde{\eta}-\Delta\tilde{\eta})$ to $\tilde{\eta}''$. At the end of "repair", the status of the cell becomes $(\tilde{N}+\Delta\tilde{N},\tilde{R}',\tilde{r}',\tilde{\eta}'',\tilde{l}''_d)$. This new state is then used as the "initial" state for the next iteration, and so forth. The dynamics of budding are summarized in Figure 2.

Finally, it is important to note that the enzymatic weakening of the cell wall (the "weaken" process, described by the parameter $\Delta\tilde{\eta}$) and the accumulation of osmolytes within the cell (the "fill" process, described by the parameter $\Delta\tilde{N}$) are two independent factors driving the whole budding process in our model. Knowing the values of $\Delta\tilde{\eta}$ and $\Delta\tilde{N}$ allows us to calculate and simulate the entire budding process. As we employed the normalized equations, we only need to know the ratio $\Delta\tilde{N}/\Delta\tilde{\eta}$ (which we denote as ψ), which determines the solution. Now, we explain how to interpret ψ: By definition, we have

$$\psi=\frac{\Delta\tilde{N}}{\Delta\tilde{\eta}}=\frac{\Delta\tilde{N}/\Delta t}{\Delta\tilde{\eta}/\Delta t}\xrightarrow{\Delta t\to 0}\frac{\dot{\tilde{N}}}{\dot{\tilde{\eta}}} \quad \text{(Equation 19)}$$

where $\dot{\tilde{N}}$ is the normalized osmolyte accumulation rate, and $\dot{\tilde{\eta}}$ is the normalized wall-weakening rate. Intuitively, ψ can thus be interpreted as how fast osmolytes accumulate inside the cell, compared to the wall-weakening process. Low ψ values mean that, compared with the wall-weakening process, $\tilde{N}$ accumulates slowly, and vice versa. To calculate the budding process, knowledge of ψ is required. In fact, ψ should be a function of time t, namely $\psi(t)$ (or a function of the iteration step i, namely ψ_i), but in this paper, we focus on the simplest scenario, assuming that ψ is a constant (the typical value of which will be discussed in detail in the third subsection in RESULTS). For a detailed discussion on ψ and how to simulate the budding process based on this model, see STAR Methods - method details (the results shown in results are all based on these simulations, and all codes are publicly available at Dryad[50]).

RESULTS

Dynamics during a cell cycle: Mother expands and shrinks

To explore the evolution of the cell wall during the progression of the cell cycle, we set $\psi=0.2$ (an arbitrary value between 0 and the maximum 1). Note that as our model did not consider the point of cytokinesis (namely, detachment), we show the budding process in a way as if cytokinesis never occurs (Figure 3). This enables us to investigate the budding process, and to "predict" when the detachment "should" occur. This is why we later observe that the daughter grows larger than the mother, although this does not occur in a normal cell cycle.

From Figure 3, we can observe that:

1. The mother's radius of curvature $\tilde{R}$ (which can be considered as the radius of the mother) increases first to a maximum value 1.1 (i.e., 10% larger than the initial radius of the mother), and then decreases, suggesting that the mother expands and then shrinks back during the cell cycle.
2. For the radius of curvature of the daughter $\tilde{r}$, we can see that beyond the critical state, $\tilde{r}$ (which can then be considered as the radius of the daughter) increases continuously, even beyond 1 where 1 represents the original radius of the mother.
3. For the osmolyte concentration difference between the inside and outside of the cell, $\tilde{C}$, we can observe that $\tilde{C}$ (also equivalent to the osmotic pressure difference $\tilde{\Pi}$, and the osmotic pressure inside the cell) first slightly increases, followed by a roughly stationary period, and then drops sharply, suggesting that when the size of the daughter $\tilde{r}$ exceeds that of the mother's, the osmotic pressure starts to drop sharply.
4. For the surface modulus of the daughter $\tilde{\eta}$: We can observe that $\tilde{\eta}$ has a similar trend as the daughter's radius of curvature ($\tilde{r}$) before a certain time point (in this case $i\approx 4300$), after which it drops sharply, though. This suggests that when the size of the daughter $\tilde{r}$ exceeds that of the mother's, the daughter's cell wall weakens sharply.

These simulations thus shows that the daughter is able to grow in size and cell wall strength. Second, although different aspects of a cell (described by different parameters and variables) are strictly constrained by physical laws and thus intricately interconnected, the cell's dynamics are governed by a single parameter ψ, namely, the ratio of the accumulation rate of osmolytes inside the cell over the rate of the wall-weakening of the daughter (referring to Equation 19). Third, the predicted cell cycle dynamics exhibit a prominent feature: the mother cell's radius (which also corresponding to its volume) first expands and then shrinks back. In the third subsection in RESULTS, after we have spanned our model's parameters and examined the bird's-eye view, we will provide an intuitive explanation for why the mother exhibits this

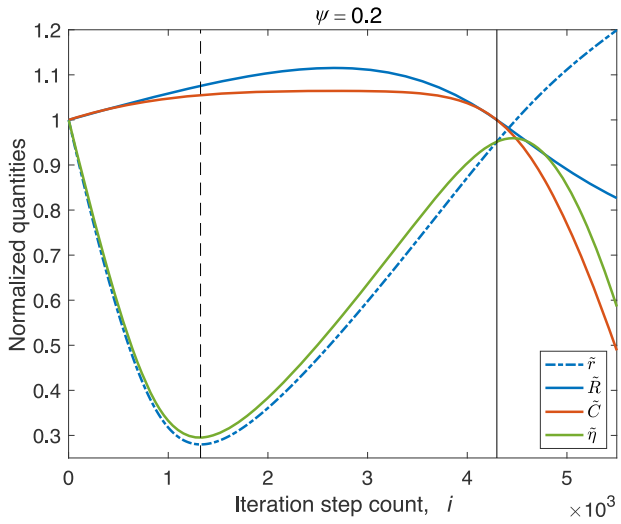

Figure 3. The dynamics of a single cell during the budding process, simulated by the model

The key parameter is set to $\psi = 0.2$, and other parameters are: $\tilde{\rho} = 0.28$, $\tilde{c}_{ex} = 0.84$ and $\tilde{V}_u = 0.4$. The figure shows the evolution of the radius of curvature of the mother ($\tilde{R}$) and the daughter ($\tilde{r}$), the surface modulus of the daughter ($\tilde{\eta}$), and the osmolyte concentration difference ($\tilde{C}$). Note that $\tilde{C}$ is always equal to the osmotic pressure difference $\tilde{\Pi}$, because from Equation 2, we can see that Π is always equal to C times a constant, so when we normalized Π to λC_0, we always have $\tilde{\Pi} = \tilde{C}$; and that this curve of $\tilde{C}$ can also represent the osmotic pressure inside the cell because the external osmotic pressure is always the same. The x axis represents the iteration step count, which is not equal to but is proportional to real-time (see STAR Methods - method details for more details). The vertical dashed line indicates the critical state. Note that before the critical state, $\tilde{r}$ first decreases to the minimum value 0.28, which is the radius of the chitin ring, $\tilde{\rho}$ (this is actually nothing special but a mathematical property because before the critical state, $\tilde{r}$ is not an indication of the daughter's size but the curvature as it is, so it must decrease till the minimum value $\tilde{\rho}$, related to Figure 1). The vertical solid line indicates the time point when the mother shrinks back to its initial size.

kind of volume oscillation behavior; and in the last subsection in RESULTS, we will provide experimental evidence that supports this prediction.

Timely detachment facilitates biophysical homeostasis

Next, we are investigating when the daughter "should" detach from the mother. The intuition is that when the daughter detaches from the mother, the status of the cell—characterized by different variables and parameters such as the radius of curvature of the mother $\tilde{R}$ and the surface modulus of the daughter $\tilde{\eta}$—"should" be unchanged compared to the initial status of the cell cycle, i.e., homeostasis should be maintained. In fact, as a whole system, these variables of the cell are interconnected and cannot change independently. It is thus not automatically guaranteed that an overall homeostasis can ever be maintained, i.e., all of these variables are kept unchanged after one cell cycle. Our model allows us to investigate this possibility quantitatively.

As we have observed in the first subsection in RESULTS, the mother's radius first increases and then decreases. With the intuition mentioned above, we hypothesize that when the mother shrinks back to its initial size, the daughter should detach from the mother (i.e., corresponding to cytokinesis). We denote this time point as DETACH, and any quantity X at this point is denoted as X_{DET}.

Now, we analyze the behaviors of the quantities at DETACH (see Figure 3 where the vertical solid line indicates DETACH):

1. For the radius of the daughter at DETACH, we observe that $\tilde{r}_{DET} = 0.95$. This value suggests an appropriate point for detachment, as it indicates the daughter is slightly smaller than the mother, allowing room for further growth. If detachment does not occur at this juncture, subsequent growth may result in the daughter surpassing the mother in size, as illustrated in Figure 3. Such a scenario is undesirable, potentially leading to progressively larger daughter cell sizes in future generations.
2. Regarding the osmolyte concentration difference at DETACH, namely, $\tilde{C}_{DET}$, we have $\tilde{C}_{DET} = 1$ exactly (equivalently, the osmotic pressure difference is always $\tilde{\Pi}_{DET} = 1$, too). This signifies an optimal detachment point, because the osmolyte concentration difference between the inside and outside of the cell (including both the mother and the daughter) remains unchanged after one cell cycle (so as the osmotic pressure difference), contributing to maintaining homeostasis.
3. For the surface modulus of the daughter at DETACH, we observe that $\tilde{\eta}_{DET}$ is nearly at its maximum, with a value of 0.95. From the aspect of the surface modulus, we could imagine that this is a good time point for detachment because: on one hand, this is the time point when the daughter's cell wall is almost the strongest ever possible (which is desirable); on the other hand, it has not surpassed the mother's strength, allowing room for further growth (otherwise, the daughter's cell wall would become stronger and stronger over generations, potentially limiting the reproductive capacity of the cells due to excessive cell wall strength).

In summary, the cell cycle dynamics, as modeled and characterized by a single governing parameter ψ, suggest that detachment at the right time (specifically, at DETACH) enables the daughter to grow to the mother's size and wall strength. Concurrently, the mother maintains

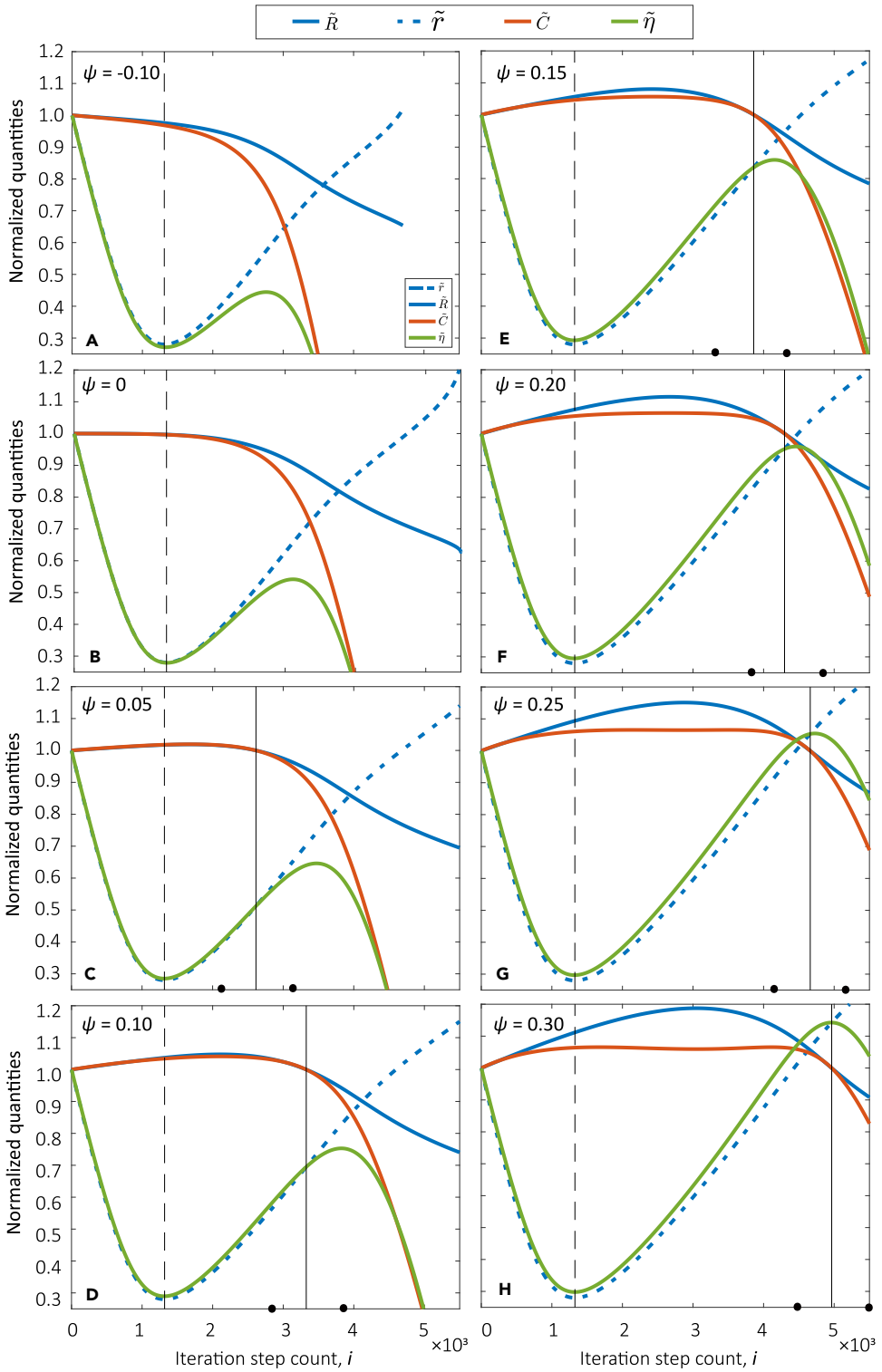

Figure 4. The dynamics of a single cell during the budding process, simulated by the model

The eight subfigures (A–H) are for eight different ψ. Other parameters are identical to that of Figure 3 (note that (F) is identical to Figure 3, shown for comparison). Each subfigure shows the evolution of the radius of curvature of the mother ($\tilde{R}$) and the daughter ($\tilde{r}$), the osmolyte concentration difference ($\tilde{C}$), and the surface modulus of the daughter ($\tilde{\eta}$). The x axis represents the iteration step count, which is not equal to but is proportional to real-time (see STAR Methods - method details for more

Figure 4. *Continued*

details). In each subfigure, the vertical dash line indicates the critical state; while the vertical solid line indicates DETACH. In (A) and (B), there are no such vertical solid lines, because the mother never shrinks back to its initial size, as per the definition of DETACH. The two black dots on the axis of each subfigure indicate two time points we chose to represent the state before and after DETACH, namely, $\pm 0.5\times 10^3$ iteration steps, referring to Figure 5.

relative stability in size, osmolyte concentration, and osmotic pressure. This indicates that, despite the stringent constraints and complex interconnections among these cellular parameters, there exists a coordination point conducive to achieving homeostasis.

An appropriate ψ is required to maintain homeostasis

Above, we have discussed the dynamics of a cell for a particular ψ. In order to have the bird's-eye view, we now set ψ to different values to investigate its effects on the cell cycle. The results are shown in Figure 4, in which we observe that:

1. As long as $\psi > 0$, the mother's radius always first increases and then shrinks back.
2. The radius of the newly-born daughter at DETACH, $\tilde{r}_{\mathrm{DET}}$, increases with ψ. When $\psi \gtrsim 0.25$, we have $\tilde{r}_{\mathrm{DET}} > 1$, i.e., the daughter is then larger than the mother.
3. The surface modulus of the newly-born daughter, $\tilde{\eta}_{\mathrm{DET}}$, increases with ψ. When $\psi \gtrsim 0.25$, we have $\tilde{\eta}_{\mathrm{DET}} > 1$, i.e., the daughter's wall strength is stronger than the mother's.
4. As long as $\psi > 0$, we always have $\tilde{C}_{\mathrm{DET}} = 1$ (equivalently $\tilde{\Pi}_{\mathrm{DET}} = 1$), i.e., the osmotic pressure of the cell stays unchanged.

Understanding the oscillation behavior of the mother cell

Now, we like to derive understanding from the model simulations, starting with the oscillation behavior of the mother cell. First, let us address why the mother cell initially expands. The enzymatic weakening of the daughter's cell wall is the first driving factor in the entire budding process. After weakening, the daughter's wall has to get more stretched (namely, more strained) to provide additional force to balance the original osmotic pressure. This increased stretching implies the growth of the daughter cell. Note that before the critical state (Figure 1B), the daughter's enlargement actually means that the value of $\tilde{r}$ decreases. This is because only after reaching the critical state, the curvature $\tilde{r}$ becomes equal to the daughter's radius, which is simply a mathematical property and not something unusual, as mentioned in the caption of Figure 3.

At this stage, the mother cell's radius $\tilde{R}$ does not have to change to achieve a new mechanical equilibrium. However, due to the influx of osmolytes ($\Delta\tilde{N} > 0$)—which increases osmolyte concentration and osmotic pressure—$\tilde{R}$ must increase to counterbalance the increased osmotic pressure. In fact, as can be seen in Figure 4B and if there is no osmolyte influx ($\Delta\tilde{N} = 0$), the mother's radius $\tilde{R}$ does not increase; and as can be seen in Figure 4A and if osmolytes flow out ($\Delta\tilde{N} < 0$), $\tilde{R}$ even decreases. Now the question is: Is the osmolyte influx essential for budding? The answer is yes. Because from Figures 4A and 4B we can see that if $\Delta\tilde{N} \not\equiv 0$, the daughter cannot grow properly. Therefore, the cell must by some means increase the concentration of osmolytes. So we can say that the mother first expands because of the influx of osmolytes, which is essential for budding. Although there have been few studies focused on the necessity of influx, a recent article[51] states that the rate of osmolyte uptake is a critical factor for cell growth: Specifically, osmolyte uptake induces water inflow, which in turn causes the cell wall to undergo elasto-plastic deformation, and without this influx, cells would not expand.

Now, let us consider why the mother cell shrinks during the later stages of the cell cycle. Likewise, firstly, the daughter's wall weakens, followed by an increase in the daughter's volume (at this stage, it has surpassed the critical point, so $\tilde{r}$ is increasing). However, as the daughter cell is already quite large, a slight increase in $\tilde{r}$ results in a significant increase in the overall cell volume. Therefore, even with a comparable influx of osmolytes as before and even with $\tilde{R}$ unchanged, it is no longer possible to prevent the osmotic pressure from decreasing. Consequently, at this stage, the radius of the mother cell, $\tilde{R}$, has to decrease to help maintain the osmotic pressure as stable as possible, in order to facilitate achieving a new mechanical equilibrium. The same logic can explain why the osmotic pressure continues to drop when the daughter becomes larger than the mother. That is, when $\tilde{r} > \tilde{R}$, even if $\tilde{R}$ decreases, it is not enough to maintain the osmotic pressure as before.

The appropriate value of ψ

To make systematic comparisons, we sketched the cell's configurations before, at, and after DETACH, under different ψ (Figure 5). We can observe that: (1) the daughter's size increases along the upper-right direction, till even larger than the mother; (2) the daughter's wall strength also increases along the upper-right direction, till even stronger than the mother (referred to the green square zones); (3) only at DETACH, the osmolyte concentration difference $\tilde{C}$ is able to stay unchanged (note that $\tilde{C}$ also represents the osmotic pressure inside the cell, as we have explained before).

The observations indicate that in order for a cell to bud properly (i.e., the daughter grows to a state similar to its mother, and the mother itself maintains homeostasis), the cell needs to "regulate" ψ to an appropriate value, but only needs to "regulate" this one parameter, that is, the ratio of the accumulation rate of osmolytes inside the cell over the rate of the wall-weakening of the daughter. If ψ is too low, the daughter cell may not grow sufficiently large, its cell wall may not be strong enough, and the mother's volume and osmotic pressure might not be maintained. Conversely, if ψ is too high, the newly born daughter cell may grow larger and have a stiffer wall than the mother, and the mother may not be able to return to its original size, thereby disrupting homeostasis over generations. Therefore, we infer that for a normal cell, ψ should be between 0.15 and 0.2. While the values 0 and 0.3 were arbitrarily chosen to span the parameter ψ's range, the "regulated" value emerges as

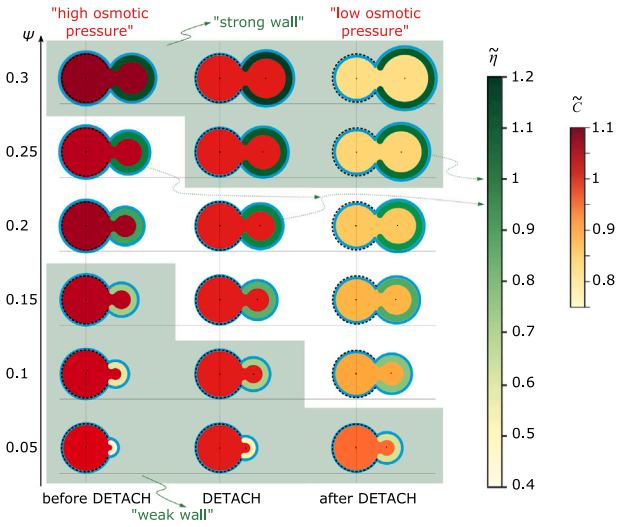

Figure 5. Diagram of the cell's configuration in different scenarios

Each cell is defined by the blue boundary. The black dashed circle on the mother side represents the original radius of the mother, namely when $\tilde{R} = 1$ (the horizontal gray thin line indicates the boundary of the mother when $\tilde{R} = 1$, for comparison across cells). The thick green circle on the daughter side represents the strength of the daughter's cell wall, η (the darker, the stronger). The red-yellow color inside the cell represents the osmolyte concentration difference, $\tilde{C}$, which can also represent the osmotic pressure inside the cell (the darker, the higher the osmotic pressure; and the six cells in the middle column always have $\tilde{C} = 1$). The upper green area marked "strong wall" indicates that η is larger than 1; while the under green area marked "weak wall" indicates that η is much smaller than 1.

a natural consequence of our model. The term "regulate" here is metaphorical; cells do not consciously regulate ψ, but it is likely an evolutionary adaptation that has positioned ψ around this value.

Experimental observations supporting model predictions

Finally, we aimed to establish links between our model predictions and experimental observations. First, our model suggests that daughter-specific cell-wall weakening is essential. Indeed, there is experimental evidence demonstrating daughter-specific processes that contribute to cellular asymmetry. For example, ASH1 mRNA is transported into the growing bud, accumulating solely in daughter cells.[52] Similarly, the Ace2 transcription factor is exclusively found in daughter cells, where it activates the expression of specific target genes.[53] Notably, among these Ace2-regulated genes are several glucanases and an endochitinase,[53] which implies that cell-wall weakening occurs primarily in daughter cells, in alignment with our model.

In this context, it is also interesting to investigate the daughter cell size upon Ace2 deletion. Here, assuming a constant osmolyte uptake rate upon Ace2 deletion, our model predicts a slightly larger daughter cell size at cytokinesis, while experimental findings indicate that the daughter cell size at cytokinesis remains unchanged compared to the wild type.[52] In this context, however, it is critical to recognize that experimentally mothers of an Ace2 deletion are larger as well.[52] This discrepancy between the model and the experiment is likely due to the fact that Ace2 also has other targets, such as Cln3, which are not captured by the model. This highlights a challenge when comparing model predictions with experimental perturbations: Experimental perturbations, such as gene deletions, often are not overly specific and often have off-target effects, or lead to cellular compensatory responses, making a comparison with the model difficult. Yet, in the context of comparing the model with the real cell, it is interesting to note that, for instance, the protein Lre1 was found to be a negative regulator of cell size,[54] and at the same time, it was found to induce accumulation of the osmolyte trehalose and to repress chitinase expression.[55] The three aspects of this protein—namely, its involvement in regulating cell size, osmolyte synthesis, and chitin/cell wall activity—are notably all at the core of our model.

Likely the best way to compare the model with reality is to look at global behavior that is predicted by the model. Here, most prominently, the model predicted oscillatory dynamics of the mother's radius (correspondingly also the cell volume), which first expands and then shrinks back (see Figure 3). Remarkably, this oscillatory behavior in the volume of the mother compartment during the cell cycle has been observed experimentally: In single-cell measurements using a microfluidic platform, Huberts et al. found volume oscillations of mother cells.[56] This finding was confirmed in a recent study, which applied machine learning tools to automatically identify individual cells. Having more reliable measurements of the volume changes in mother cells during cell cycles, this study also revealed volume oscillations of the mother cell.[57] Interestingly, it was also reported that mother cells after every daughter division do not fully shrink back to the original size, meaning that the mother gets larger and larger with "reproductive age".[56] This suggests that in reality yeast cells do not manage to accomplish full homeostasis. Also, this aspect can be captured by our model. If one assumes that cytokinesis does occur slightly before what we defined as the optimal point from a homeostasis point of view (referring to the left of the black solid lines in Figure 4), we can see that the mother cell is slightly larger than it is prior to budding.

Finally, in the third subsection in RESULTS, we argued that we would expect ψ to be in a range of 0.15 and 0.2, as this range allows cells to maintain homeostasis over generations. Within this range of ψ value, our model predicts that, when going from 0.15 to 0.2, the volume of daughters would vary by 39.6% at cytokinesis (see STAR Methods - method details). Interestingly, this range of daughter cell size variation is also found in experiments. Specifically, it was found that in a yeast wildtype grown on glucose, the daughter cell size at cytokinesis varies 44% considering the interquartile range of the measured cell size distribution.[58] Thus, taken together, decent agreement exists between our model predictions and experimental observations.

DISCUSSION

In the model developed in this paper, we linked Newtonian mechanics over the cell wall and the biochemical processes that change the mechanical properties of the wall together (which leads to budding) in a quantitative manner. Our model reproduces experimentally observed behavior without fitting. In specific, our work suggests that the asymmetry of cell division is a prerequisite for the daughter cell to sustain budding-compatible mechanical stiffness, and the "expand and then shrink" behavior of the mother is an inevitable consequence of the budding mechanism. This "expand and then shrink" behavior is consistent with empirical observations in the literature,[56,57] suggesting that our model captures the mechanisms of the budding process correctly.

Our model demonstrates important homeostatic features. In specific, although various variables of the cell (such as osmotic pressure, wall strength, and size) are strictly constrained and intricately interconnected, there is an appropriate time point when they are desirably coordinated so that homeostasis can be automatically achieved. Our model suggests that this time point is when the mother shrinks back to its original size, and it is also when the daughter is slightly smaller than the mother. This gives a mechanism-based explanation of why the daughter needs to detach when it is smaller than the mother, i.e., asymmetric division.

Moreover, we found that in order for a cell to bud appropriately, the cell needs to "regulate" one parameter—ψ, the ratio of the accumulation rate of osmolytes inside the cell over the rate of the wall-weakening of the daughter—to an appropriate value, which also implies that we can manipulate ψ to regulate a cell's budding process. Cell wall weakening has been shown to occur via cell-wall degrading enzymes such as Gas1 (a glycosyl-phosphatidylinositol-anchored plasma membrane protein[59,60]) and the proteins belonging to the Bg12 family of endo-beta-1,3-glucanases.[15,38,61] In turn, recent findings suggest that certain biosynthetic processes are temporally segregated during the budding yeast cell cycle.[62] We envision that such segregation could control the rate of osmolyte accumulation. Together, the regulated activity of cell-wall degrading enzymes and the temporally altering biosynthetic processes influencing the rate of osmolyte accumulation could set the right ratio ψ for the cell budding process.

In conclusion, our model recapitulates the evolution of mother- and daughter-specific dynamics of cell size, as defined by continuous single-cell measurements, providing a quantitative tool to investigate the mechanisms linking observable phenotypic features and mechanics of the cell with various internal molecular processes. This quantitative description of how the cell wall evolves could provide valuable insights into cell morphology from a system perspective.

Limitations of the study

Several limitations should be elucidated. Our model primarily considers how osmotic effects and their coupling with cell wall synthesis govern cell budding. While it successfully predicts often-overlooked oscillatory size changes in mother cells during budding, certain mechanisms affecting cell morphology, such as the cytoskeleton, were neglected. These factors should be considered in the future, especially if more precise predictions are needed. Meanwhile, perturbation experiments (e.g., altering genes involved in cell wall synthesis or intentionally changing osmotic pressure) are highly desirable. These would help further validate the model and identify key factors influencing cell division, facilitating the manipulation of the cell cycle.

RESOURCE AVAILABILITY

Lead contact

Further information and requests for resources should be directed to and will be fulfilled by the lead contact, Y.L. (yu.ernest.liu@bnu.edu.cn).

Materials availability

This study did not generate new unique materials.

Data and code availability

- All data have been deposited at Dryad and are publicly available as of the date of publication. Accession numbers are listed in the key resources table.
- All code has been deposited at Dryad and is publicly available as of the date of publication. Accession numbers are listed in the key resources table.
- Any additional information required to reanalyze the data reported in this paper is available from the lead contact upon request.

ACKNOWLEDGMENTS

This work was funded by the National Natural Science Foundation of China (Grant No. 12205012 to Y.L. and 11971405 to D.Z.), Beijing Normal University via the Youth Talent Strategic Program (Grant No. 28705-310432106 to Y.L.), Advanced Institute of Natural Sciences at Beijing Normal University via the Incubation Project for Interdisciplinary Research (to Y.L.), the Fundamental Research Funds for the Central Universities (No. 20720230023 to D.Z.), and the "BaSyC—Building a Synthetic Cell" Gravitation grant (No. 024.003.019 to M.H.) of the Netherlands Ministry of Education, Culture, and Science (OCW) and the Dutch Research Council

(NWO). The funders had no role in study design, data collection and analysis, decision to publish, or preparation of the manuscript. We thank Dr. Athanasios Litsios for the fruitful discussions and insightful comments.

AUTHOR CONTRIBUTIONS

Conceptualization, Y.L. and M.H.; methodology, Y.L., C.L., and M.H.; software, Y.L., C.L., S.T., Y.P., X.W., and L.Q.; validation, Y.L., C.L., S.T., H.X., X.W., Y.P., X.W., and L.Q.; formal analysis, Y.L., C.L., S.T., H.X., X.W., Y.P., X.W., and L.Q.; investigation, Y.L., C.L., S.T., H.X., X.W., Y.P., X.W., and L.Q.; resources, Y.L., C.L., Z.D., D.Z., and M.H.; data curation, Y.L. and C.L.; writing—original draft preparation, all authors; writing—review and editing, Y.L., C.L., and M.H.; visualization, Y.L., C.L., and S.T.; supervision, Y.L., Z.D., D.Z., and M.H.; project administration, Y.L., Z.D., and M.H.; funding acquisition, Y.L., D.Z. and M.H. All authors have read and agreed to the published version of the manuscript.

DECLARATION OF INTERESTS

The authors declare no competing interests.

STAR★METHODS

Detailed methods are provided in the online version of this paper and include the following:

- KEY RESOURCES TABLE
- METHOD DETAILS
  - More empirical evidence for model assumptions
  - "Weaken-fill-repair" and "pump-leak"
  - Mechanical equations for the daughter
  - Normalization for equations of the cell
  - Reference values for normalization
  - Implementation of the model
  - Meaning of "iteration step" in the model
  - Daughter cell size variation
  - Abnormalities in wall integrity pathway
  - Effects of osmotic pressure
- QUANTIFICATION AND STATISTICAL ANALYSIS

SUPPLEMENTAL INFORMATION

Supplemental information can be found online at https://doi.org/10.1016/j.isci.2024.110981.

Received: February 8, 2024
Revised: June 8, 2024
Accepted: September 13, 2024
Published: September 18, 2024

REFERENCES

1. Litsios, A., Huberts, D.H.E.W., Terpstra, H.M., Guerra, P., Schmidt, A., Buczak, K., Papagiannakis, A., Rovetta, M., Hekelaar, J., Hubmann, G., et al. (2019). Differential scaling between g1 protein production and cell size dynamics promotes commitment to the cell division cycle in budding yeast. Nat. Cell Biol. *21*, 1382–1392.
2. Papagiannakis, A., Niebel, B., Wit, E.C., and Heinemann, M. (2017). Autonomous metabolic oscillations robustly gate the early and late cell cycle. Mol. Cell *65*, 285–295.
3. Li, F., Long, T., Lu, Y., Ouyang, Q., and Tang, C. (2004). The yeast cell-cycle network is robustly designed. Proc. Natl. Acad. Sci. USA *101*, 4781–4786.
4. Tu, B.P., Kudlicki, A., Rowicka, M., and McKnight, S.L. (2005). Logic of the yeast metabolic cycle: temporal compartmentalization of cellular processes. Science *310*, 1152–1158.
5. Chang, F. (2017). Forces that shape fission yeast cells. Mol. Biol. Cell *28*, 1819–1824.
6. Tsai, K., Britton, S., Nematbakhsh, A., Zandi, R., Chen, W., and Alber, M. (2020). Role of combined cell membrane and wall mechanical properties regulated by polarity signals in cell budding. Phys. Biol. *17*, 065011.
7. Bashirzadeh, Y., Moghimianavval, H., and Liu, A.P. (2022). Encapsulated actomyosin patterns drive cell-like membrane shape changes. iScience *25*, 104236.
8. Venkova, L., Vishen, A.S., Lembo, S., Srivastava, N., Duchamp, B., Ruppel, A., Williart, A., Vassilopoulos, S., Deslys, A., Garcia Arcos, J.M., et al. (2022). A mechano-osmotic feedback couples cell volume to the rate of cell deformation. Elife *11*, e72381.
9. Chang, F., and Huang, K.C. (2014). How and why cells grow as rods. BMC Biol. *12*, 54.
10. Davì, V., and Minc, N. (2015). Mechanics and morphogenesis of fission yeast cells. Curr. Opin. Microbiol. *28*, 36–45.
11. Rojas, E.R., Hotton, S., and Dumais, J. (2011). Chemically Mediated Mechanical Expansion of the Pollen Tube Cell Wall. Biophys. J. *101*, 1844–1853.
12. Bernal, R., Rojas, E., and Dumais, J. (2007). The mechanics of tip growth morphogenesis: what we have learned from rubber balloons. J. Mech. Mater. Struct. *2*, 1157–1168.
13. Rojas, E.R., and Huang, K.C. (2018). Regulation of microbial growth by turgor pressure. Curr. Opin. Microbiol. *42*, 62–70.
14. Rojas, E.R., Billings, G., Odermatt, P.D., Auer, G.K., Zhu, L., Miguel, A., Chang, F., Weibel, D.B., Theriot, J.A., and Huang, K.C. (2018). The outer membrane is an essential load-bearing element in Gram-negative bacteria. Nature *559*, 617–621.
15. Vermassen, A., Leroy, S., Talon, R., Provot, C., Popowska, M., and Desvaux, M. (2019). Cell wall hydrolases in bacteria: insight on the diversity of cell wall amidases, glycosidases and peptidases toward peptidoglycan. Front. Microbiol. *10*, 331.
16. Smith, A.E., Zhang, Z., Thomas, C.R., Moxham, K.E., and Middelberg, A.P. (2000a). The mechanical properties of Saccharomyces cerevisiae. Proc. Natl. Acad. Sci. USA *97*, 9871–9874.
17. Alsteens, D., Dupres, V., Mc Evoy, K., Wildling, L., Gruber, H.J., and Dufrêne, Y.F. (2008). Structure, cell wall elasticity and polysaccharide properties of living yeast cells, as probed by AFM. Nanotechnology *19*, 384005.
18. Smith, A., Zhang, Z., and Thomas, C. (2000b). Wall material properties of yeast cells: Part 1. Cell measurements and compression experiments. Chem. Eng. Sci. *55*, 2031–2041.
19. Minc, N., Boudaoud, A., and Chang, F. (2009). Mechanical Forces of Fission Yeast Growth. Curr. Biol. *19*, 1096–1101.
20. Proseus, T.E., Ortega, J.K., and Boyer, J.S. (1999). Separating growth from elastic deformation during cell enlargement. Plant Physiol. *119*, 775–784.
21. Goldenbogen, B., Giese, W., Hemmen, M., Uhlendorf, J., Herrmann, A., and Klipp, E.

(2016). Dynamics of cell wall elasticity pattern shapes the cell during yeast mating morphogenesis. Open Biol. *6*, 160136.
22. Schaber, J., Adrover, M.A., Eriksson, E., Pelet, S., Petelenz-Kurdziel, E., Klein, D., Posas, F., Goksör, M., Peter, M., Hohmann, S., and Klipp, E. (2010a). Biophysical properties of saccharomyces cerevisiae and their relationship with hog pathway activation. Eur. Biophys. J. *39*, 1547–1556.
23. Midtvedt, D., Olsén, E., Höök, F., and Jeffries, G.D.M. (2019). Label-free spatio-temporal monitoring of cytosolic mass, osmolarity, and volume in living cells. Nat. Commun. *10*, 340.
24. Jiang, S., Ma, Y., and Dai, J. (2024). Synthetic yeast genome project and beyond. Innov. Life *2*, 100059.
25. Jan, Y.N., and Jan, L.Y. (1998). Asymmetric cell division. Nature *392*, 775–778.
26. Sunchu, B., and Cabernard, C. (2020). Principles and mechanisms of asymmetric cell division. Development *147*, dev167650.
27. LeGoff, L., and Lecuit, T. (2015). Mechanical forces and growth in animal tissues. Cold Spring Harbor Perspect. Biol. *8*, a019232.
28. Rivera-Yoshida, N., Arias Del Angel, J.A., and Benítez, M. (2018). Microbial multicellular development: mechanical forces in action. Curr. Opin. Genet. Dev. *51*, 37–45.
29. Drake, T., and Vavylonis, D. (2013). Model of Fission Yeast Cell Shape Driven by Membrane-Bound Growth Factors and the Cytoskeleton. PLoS Comput. Biol. *9*, e1003287.
30. Wong, F., Garner, E.C., and Amir, A. (2019). Mechanics and dynamics of translocating mreb filaments on curved membranes. Elife *8*, e40472.
31. Dumais, J., Shaw, S.L., Steele, C.R., Long, S.R., and Ray, P.M. (2006). An anisotropic-viscoplastic model of plant cell morphogenesis by tip growth. Int. J. Dev. Biol. *50*, 209–222.
32. Lai, H., Chiou, J.-G., Zhurikhina, A., Zyla, T.R., Tsygankov, D., and Lew, D.J. (2018). Temporal regulation of morphogenetic events in saccharomyces cerevisiae. Mol. Biol. Cell *29*, 2069–2083.
33. Chowdhury, S., Smith, K.W., and Gustin, M.C. (1992). Osmotic stress and the yeast cytoskeleton: phenotype-specific suppression of an actin mutation. J. Cell Biol. *118*, 561–571.
34. Rojas, E.R., Huang, K.C., and Theriot, J.A. (2017). Homeostatic Cell Growth Is Accomplished Mechanically through Membrane Tension Inhibition of Cell-Wall Synthesis. Cell Syst. *5*, 578–590.e6.
35. Orlean, P. (2012). Architecture and Biosynthesis of the *Saccharomyces cerevisiae* Cell Wall. Genetics *192*, 775–818.
36. Tkacz, J.S., and Lampen, J.O. (1972). Wall replication in saccharomyces species: use of fluorescein-conjugated concanavalin a to reveal the site of mannan insertion. Microbiology *72*, 243–247.
37. Cosgrove, D.J. (2000). Loosening of plant cell walls by expansins. Nature *407*, 321–326.
38. Adams, D.J. (2004). Fungal cell wall chitinases and glucanases. Microbiology *150*, 2029–2035.
39. Aminzare, Z., and Kay, A.R. (2022). Mathematical modeling of ion homeostasis & cell volume stabilization: impact of ion transporters, impermeant molecules, & donnan effect. Preprint at bioRxiv *2022–12*. https://doi.org/10.1101/2022.12.08.519683.
40. Kay, A.R., and Blaustein, M.P. (2019). Evolution of our understanding of cell volume regulation by the pump-leak mechanism. J. Gen. Physiol. *151*, 407–416.
41. Xie, S., Swaffer, M., and Skotheim, J.M. (2022). Eukaryotic cell size control and its relation to biosynthesis and senescence. Annu. Rev. Cell Dev. Biol. *38*, 291–319.
42. Lanz, M.C., Zatulovskiy, E., Swaffer, M.P., Zhang, L., Ilerten, I., Zhang, S., You, D.S., Marinov, G., McAlpine, P., Elias, J.E., and Skotheim, J.M. (2022). Increasing cell size remodels the proteome and promotes senescence. Mol. Cell *82*, 3255–3269.e8.
43. Tiruvadi-Krishnan, S., Männik, J., Kar, P., Lin, J., Amir, A., and Männik, J. (2022). Coupling between dna replication, segregation, and the onset of constriction in Escherichia coli. Cell Rep. *38*, 110539.
44. Barber, F., Amir, A., and Murray, A.W. (2020). Cell-size regulation in budding yeast does not depend on linear accumulation of whi5. Proc. Natl. Acad. Sci. USA *117*, 14243–14250.
45. Soifer, I., Robert, L., and Amir, A. (2016). Single-cell analysis of growth in budding yeast and bacteria reveals a common size regulation strategy. Curr. Biol. *26*, 356–361.
46. Zatulovskiy, E., and Skotheim, J.M. (2020). On the molecular mechanisms regulating animal cell size homeostasis. Trends Genet. *36*, 360–372.
47. Goodno, B.J., and Gere, J.M. (2020). Mechanics of Materials (Cengage learning).
48. Atkins, P., and Paula, J.d. (2014). Physical Chemistry Thermodynamics, Structure, and Change (New York: WH Freeman and Company).
49. Smith, A., Moxham, K., and Middelberg, A. (1998). On uniquely determining cell–wall material properties with the compression experiment. Chem. Eng. Sci. *53*, 3913–3922.
50. Liu, Y., Liu, C., Tang, S., Xiao, H., Wu, X., Peng, Y., Wang, X., Que, L., Di, Z., Zhou, D., and Heinemann, M. (2023). Code for the article "The weaken-fill-repair" model for cell budding: Linking cell wall biosynthesis with mechanics. Dryad. https://doi.org/10.5061/dryad.qjq2bvqn0.
51. Altenburg, T., Goldenbogen, B., Uhlendorf, J., and Klipp, E. (2019). Osmolyte homeostasis controls single-cell growth rate and maximum cell size of saccharomyces cerevisiae. NPJ Syst. Biol. Appl. *5*, 34.
52. Di Talia, S., Wang, H., Skotheim, J.M., Rosebrock, A.P., Futcher, B., and Cross, F.R. (2009). Daughter-specific transcription factors regulate cell size control in budding yeast. PLoS Biol. *7*, e1000221.
53. Teixeira, M.C., Viana, R., Palma, M., Oliveira, J., Galocha, M., Mota, M.N., Couceiro, D., Pereira, M.G., Antunes, M., Costa, I.V., et al. (2023). YEASTRACT+: a portal for the exploitation of global transcription regulation and metabolic model data in yeast biotechnology and pathogenesis. Nucleic Acids Res. *51*, D785–D791.
54. Soifer, I., and Barkai, N. (2014). Systematic identification of cell size regulators in budding yeast. Mol. Syst. Biol. *10*, 761.
55. Versele, M., and Thevelein, J.M. (2001). Lre1 affects chitinase expression, trehalose accumulation and heat resistance through inhibition of the cbk1 protein kinase in saccharomyces cerevisiae. Mol. Microbiol. *41*, 1311–1326.
56. Huberts, D. (2015). The Impact of Metabolism on Aging and Cell Size in Single Yeast Cells (Ph.D. thesis University of Groningen).
57. Pietsch, J.M.J., Muñoz, A.F., Adjavon, D.-Y.A., Farquhar, I., Clark, I.B.N., and Swain, P.S. (2023). Determining growth rates from bright-field images of budding cells through identifying overlaps. Elife *12*, e79812.
58. Novarina, D., Guerra, P., and Milias-Argeitis, A. (2021). Vacuolar localization via the n-terminal domain of sch9 is required for torc1-dependent phosphorylation and downstream signal transduction. J. Mol. Biol. *433*, 167326.
59. Popolo, L., and Vai, M. (1999). The gas1 glycoprotein, a putative wall polymer cross-linker. Biochim. Biophys. Acta *1426*, 385–400.
60. Klis, F.M., Boorsma, A., and De Groot, P.W.J. (2006). Cell wall construction in saccharomyces cerevisiae. Yeast *23*, 185–202.
61. Baladrón, V., Ufano, S., Dueñas, E., Martín-Cuadrado, A.B., del Rey, F., and Vázquez de Aldana, C.R. (2002). Eng1p, an endo-1, 3-β-glucanase localized at the daughter side of the septum, is involved in cell separation in saccharomyces cerevisiae. Eukaryot. Cell *1*, 774–786.
62. Takhaveev, V., Özsezen, S., Smith, E.N., Zylstra, A., Chaillet, M.L., Chen, H., Papagiannakis, A., Milias-Argeitis, A., and Heinemann, M. (2023). Temporal segregation of biosynthetic processes is responsible for metabolic oscillations during the budding yeast cell cycle. Nat. Metab. *5*, 294–313.
63. Blatzer, M., Beauvais, A., Henrissat, B., and Latgé, J.-P. (2020). Revisiting Old Questions and New Approaches to Investigate the Fungal Cell Wall Construction (Springer International Publishing), pp. 331–369.
64. Cabib, E., Farkas, V., Kosík, O., Blanco, N., Arroyo, J., and McPhie, P. (2008). Assembly of the yeast cell wall: Crh1p and crh2p act as transglycosylases in vivo and in vitro. J. Biol. Chem. *283*, 29859–29872.
65. Lesage, G., and Bussey, H. (2006). Cell wall assembly in saccharomyces cerevisiae. Microbiol. Mol. Biol. Rev. *70*, 317–343.
66. Smits, G.J., Kapteyn, J.C., van den Ende, H., and Klis, F.M. (1999). Cell wall dynamics in yeast. Curr. Opin. Microbiol. *2*, 348–352.
67. Chung, K.L., Hawirko, R.Z., and Isaac, P.K. (1965). Cell wall replication in saccharomyces cerevisiae. Can. J. Microbiol. *11*, 953–957.
68. Proctor, S.A., Minc, N., Boudaoud, A., and Chang, F. (2012). Contributions of turgor pressure, the contractile ring, and septum assembly to forces in cytokinesis in fission yeast. Curr. Biol. *22*, 1601–1608.
69. Rodríguez-Peña, J.M., Cid, V.J., Arroyo, J., and Nombela, C. (2000). A novel family of cell wall-related proteins regulated differently during the yeast life cycle. Mol. Cell Biol. *20*, 3245–3255.
70. Gervais, P., and Beney, L. (2001). Osmotic mass transfer in the yeast saccharomyces cerevisiae. Cell. Mol. Biol. *47*, 831–839.
71. Zhang, J., Schneider, C., Ottmers, L., Rodriguez, R., Day, A., Markwardt, J., and Schneider, B.L. (2002). Genomic scale mutant hunt identifies cell size homeostasis genes in s. cerevisiae. Curr. Biol. *12*, 1992–2001.
72. Levin, D.E. (2005). Cell wall integrity signaling in saccharomyces cerevisiae. Microbiol. Mol. Biol. Rev. *69*, 262–291.
73. Klipp, E., Nordlander, B., Krüger, R., Gennemark, P., and Hohmann, S. (2005). Integrative model of the response of yeast to osmotic shock. Nat. Biotechnol. *23*, 975–982.

74. Hohmann, S. (2002). Osmotic stress signaling and osmoadaptation in yeasts. Microbiol. Mol. Biol. Rev. *66*, 300–372.
75. Mager, W.H., and Siderius, M. (2002). Novel insights into the osmotic stress response of yeast. FEMS Yeast Res. *2*, 251–257.
76. Radmaneshfar, E., Kaloriti, D., Gustin, M.C., Gow, N.A.R., Brown, A.J.P., Grebogi, C., Romano, M.C., and Thiel, M. (2013). From start to finish: The influence of osmotic stress on the cell cycle. PLoS One *8*, e68067.
77. Schaber, J., Adrover, M.A., Eriksson, E., Pelet, S., Petelenz-Kurdziel, E., Klein, D., Posas, F., Goksör, M., Peter, M., Hohmann, S., and Klipp, E. (2010b). Biophysical properties of saccharomyces cerevisiae and their relationship with hog pathway activation. Eur. Biophys. J. *39*, 1547–1556.
78. Duveau, F., Cordier, C., Chiron, L., Le Bec, M., Pouzet, S., Séguin, J., Llamosi, A., Sorre, B., Di Meglio, J.M., and Hersen, P. (2024). Yeast cell responses and survival during periodic osmotic stress are controlled by glucose availability. Elife *12*, RP88750.

STAR★METHODS

KEY RESOURCES TABLE

REAGENT or RESOURCE	SOURCE	IDENTIFIER
Deposited data		
Code and data for development and evaluation	This paper	Dryad: https://datadryad.org/stash/dataset/doi:10.5061/dryad.qjq2bvqn0
Software and algorithms		
MATLAB R2020b or above	MATLAB Software Foundation	https://www.mathworks.com/products/matlab.html

METHOD DETAILS

More empirical evidence for model assumptions

There are various empirical observations for cell wall expansion and budding: (1) To initiate the budding, the cell wall of the bud region has to be weakened to some extent.[6,32] (2) The wall weakening is observed to be processed by wall-degrading enzymes such as Gas1[59,60] and the proteins belonging to the Bg12 family of endo-beta-1,3-glucanases.[15,38,61] (3) The concept that the growing cell wall must be "loosened" (or weakened) to expand its surface is derived from various biophysical, biochemical, and physiological considerations. This idea has been around for quite a while.[37] In yeast, the polysaccharide cross-linking necessary to assemble the new fungal cell wall requires a mechanism in which, for every new link formed, an existing link must be broken, allowing for the absence of free energy sources outside the plasma membrane.[38] During yeast growth and division, the cell wall is a highly dynamic structure subject to constant change.[63] In the budding process of yeast, several proteins are primarily expressed and active on the daughter cell side, where they participate in the hydrolysis or remodeling of the cell wall. A notable example includes Crh1p and Crh2p, two transglycosylases; these enzymes assist in local cell wall remodeling by modifying β-1,3-glucan and chitin. Additionally, Chs3p is another critical protein that is mainly expressed at the bud site during budding, responsible for chitin synthesis, thereby influencing the structure and function of the cell wall.[64,65]

(4) Weakening of the cell wall activates a cell wall integrity pathway, leading to compensatory changes in the wall and a balance between the wall degradation and the biosynthesis.[15,66] This is further supported by the fact that the mechanical stress on the cell wall can be sensed by sensor membrane proteins, for which the Wsc and Mid proteins are potential candidates.[35,66] (5) The cell wall materials are integrated almost exclusively into the daughter and not into the mother.[36,67] (6) Turgor pressure is defined to be the mechanical force that pushes the membrane against the wall.[6] In mechanical equilibrium, turgor pressure is balanced by the osmotic pressure, which is linearly correlated with the osmolyte (including various small molecules such as glucose and amino acids) concentration difference inside and outside of the cell. Previous studies showed that the turgor pressure of the mother almost stays constant during the cell cycle.[21,22,68] Based on these observations, we made several reasonable assumptions, and then we derived our quantitative model.

"Weaken-fill-repair" and "pump-leak"

The "pump and leak" model (or "pump-leak" mechanism, PLM) is a classic model that explains how the osmotic balance stabilizes cell volume. Yet, there are several significant differences between PLM and our "weaken-fill-repair" model, although there is no conflict. The key distinctions are: 1. PLM primarily addresses animal cells, which lack cell walls. It focuses on the balance across the cell membrane. But in our model, we have to take into account the mechanical properties of the cell wall, which differ significantly from those of the membrane. For instance, the wall is extensible and can be viewed as incompressible, capable of providing considerable force (namely, mechanical stress), unlike the "soft" membrane, which offers limited stress. 2. In PLM, given the relative "softness" of the membrane, cells need to regulate their internal ion concentration and volume to prevent excessive swelling or shrinkage due to osmotic pressure differences; then, mechanical equilibrium is largely a matter of osmotic balance on both sides of the membrane. However, in cells with a wall, the internal and external osmotic pressure can be very different, making it necessary to consider the force provided by the wall. 3. Our model specifically examines the budding process in yeast, involving a very rigid chitin ring on the mother cell's neck, the enzymatic weakening of the cell wall inside the ring (altering its mechanical properties) to enable growth, among other factors. These aspects are not considered in PLM.

In fact, any substance that can affect the osmotic pressure of a cell is termed an osmolyte, which includes ions as well as other small molecules such as various amino acids, glycerol, ATP, and small nucleotides. These osmolytes are key factors affecting the osmotic pressure. In our model, the variable N represents the total osmolyte amount inside the cell, as described in Equation 2. On the other hand, the key parameter of our model, ψ, which significantly influences the entire budding process, is defined as Equation 19, and $\Delta\tilde{N}$ is the osmolyte accumulation rate. Thus, from this perspective, our model does consider ions (as it considers osmolytes as a whole). The mechanical equilibrium of the cell wall is derived from the interaction between the osmotic pressure produced by osmolytes and the mechanical stress exerted by the cell wall. This is the foundation that allows us to formulate Equation 1 and, from there, derive the fundamental equations in our model, Equations 11 and 12.

Mechanical equations for the daughter

Note that, although in Equation 3 we have taken a small element on the mother's wall as an example, the same principle also applies to the daughter. Now, we derive the Newtonian equations for the daughter. We rewrite Equation 3 specifically for an element from the daughter:

$$(\lambda C \cdot r / 2 - \sigma_d h_d) \cdot r = M_d a_d / (2\pi) \quad \text{(Equation 20)}$$

The subscript d represents the quantities from the daughter. Note that in the process of budding, there will be new wall materials integrated into the daughter's wall, so unlike the mother, the mechanical properties of the daughter are subject to change. Nevertheless, we can assume that between the time interval in which no new material is integrated, the daughter's wall is completely linear-elastic and isotropic. So we can still use the Lagrangian strain and apply Hooke's law to this element:

$$\epsilon_d(r, l_d) = L_d(r) / l_d - 1 \quad \text{(Equation 21)}$$

$$\sigma_d = k_d \cdot \epsilon_d(r, l_d) \quad \text{(Equation 22)}$$

where ϵ_d is the Lagrangian strain of this element, L_d is the stretched circumference of daughter, and l_d is the unstretched circumference. Unlike l_m, here l_d is no longer a constant (that is why ϵ_d is a function of both r and l_d), but it changes as new wall materials are integrated into. In this way, the biosynthesis of wall materials is taken into account.

At the initial state (Figure 1B), the mechanical equilibrium described by Equation 7 also applies to the daughter. Therefore, we can incorporate Equations 7, 21, and 22 into Equation 20, and then we have

$$\left(\frac{C}{C_0}\frac{r}{R_0} - \frac{k_d h_d}{k_m h_{m0}}\frac{\epsilon_d}{\epsilon_{m0}}\right) \cdot \frac{r}{R_0} = \frac{a_d}{\pi\lambda C_0 R_0^2 / M_d}$$

For convenience, we rewrite $k_d h_d$ as a single variable η [N/m] which corresponds to the so-called surface modulus, representing the "strength" of the daughter's wall[16]; and let $\eta_0 \equiv k_m h_{m0}$. Then, we obtain the overall Equation 23 for Newtonian mechanics of the daughter:

$$\left(\frac{C}{C_0}\frac{r}{R_0} - \frac{\eta}{\eta_0}\frac{\epsilon_d}{\epsilon_{m0}}\right) \cdot \frac{r}{R_0} = \frac{a_d}{\pi\lambda C_0 R_0^2 / M_d} \quad \text{(Equation 23)}$$

Normalization for equations of the cell

(1) First of all, we normalize every geometric quantity to a specific initial value.
   (a) We normalize the mother's and the daughter's radius of curvature R and r to R_0, that is, let $\tilde{R} \equiv R/R_0$ and $\tilde{r} \equiv r/R_0$. The superscript tilde ~ always represents a normalized quantity.
   (b) We normalize the circumference of the mother:

$$\tilde{L}_m(\tilde{R}) = \frac{L_m(R)}{R_0} = \frac{2R \cdot [\pi - \arcsin(\rho/R)]}{R_0} = 2\frac{R}{R_0} \cdot \left[\pi - \arcsin\frac{\rho/R_0}{R/R_0}\right]$$
$$= 2\tilde{R} \cdot [\pi - \arcsin(\tilde{\rho}/\tilde{R})]$$

Then, we normalize the circumference of the daughter, which is a step-wise function. Before the critical state,

$$\tilde{L}_{d1}(\tilde{r}) = \frac{L_{d1}(r)}{R_0} = \frac{2r \cdot \arcsin(\rho/r)}{R_0} = 2\tilde{r} \cdot \arcsin(\tilde{\rho}/\tilde{r})$$

while after the critical state,

$$\tilde{L}_{d2}(\tilde{r}) = \frac{L_{d2}(r)}{R_0} = \frac{2r \cdot [\pi - \arcsin(\rho/r)]}{R_0} = 2\frac{r}{R_0} \cdot \left[\pi - \arcsin\frac{\rho/R_0}{r/R_0}\right]$$
$$= 2\tilde{r} \cdot [\pi - \arcsin(\tilde{\rho}/\tilde{r})]$$

In summary,

$$\tilde{L}_d(\tilde{r}) = \begin{cases} \tilde{L}_{d1}(\tilde{r}), \text{if before the critical state,} \\ \tilde{L}_{d2}(\tilde{r}), \text{if after the critical stat} \end{cases}$$

   (c) We normalize the surface area of the mother,

$$\tilde{S}_m(\tilde{R}) = \frac{S_m(R)}{S_{m0}} = \frac{2\pi R\left(R+\sqrt{R^2-\rho^2}\right)}{2\pi R_0\left(R_0+\sqrt{R_0^2-\rho^2}\right)} = \frac{R}{R_0}\cdot\frac{R\Big/R_0+\sqrt{(R/R_0)^2-(\rho/R_0)^2}}{1+\sqrt{1-(\rho/R_0)^2}}$$
$$= \tilde{R}\cdot\frac{\tilde{R}+\sqrt{\tilde{R}^2-\tilde{\rho}^2}}{1+\sqrt{1-\tilde{\rho}^2}} = \tilde{R}^2\cdot\frac{1+\sqrt{1-(\tilde{\rho}/\tilde{R})^2}}{1+\sqrt{1-\tilde{\rho}^2}}$$

As in Equation 23 the surface area of the daughter does not appear, there is nothing to normalize.

(d) We normalize the total volume of the cell, which is a piece-wise function. Before the critical state, the total volume is (note that if $F(x,y)$ is a function of x and y, we denote the reference value $F_0 \equiv F(x_0,y_0)$):

$$\tilde{V}_1(\tilde{R},\tilde{r}) = \frac{V_1(R,r)}{V_0} = \left[\left(\frac{2}{3}-\frac{\beta_m^3}{3}+\beta_m\right)\pi R^3+\frac{4}{3}\pi r^3-\left(\frac{2}{3}-\frac{\beta_d^3}{3}+\beta_d\right)\pi r^3\right]\Big/\left(\frac{4}{3}\pi R_0^3\right)$$
$$= \left[\left(\frac{2}{3}-\frac{\beta_m^3}{3}+\beta_m\right)\left(\frac{R}{R_0}\right)^3+\frac{4}{3}\left(\frac{r}{R_0}\right)^3-\left(\frac{2}{3}-\frac{\beta_d^3}{3}+\beta_d\right)\left(\frac{r}{R_0}\right)^3\right]\cdot\frac{3}{4}$$
$$= \tilde{R}^3\cdot\left[\left(\frac{1}{2}-\frac{\beta_m^3}{4}+\frac{3\beta_m}{4}\right)+\left(\frac{1}{2}+\frac{\beta_d^3}{4}-\frac{3\beta_d}{4}\right)\left(\frac{\tilde{r}}{\tilde{R}}\right)^3\right]$$

where

$$\begin{cases}\beta_m = \sqrt{R^2-\rho^2}\Big/R = \sqrt{1-(\tilde{\rho}/\tilde{R})^2}\\ \beta_d = \sqrt{r^2-\rho^2}\Big/r = \sqrt{1-(\tilde{\rho}/\tilde{r})^2}\end{cases}$$

while after the critical state, the total volume is

$$\tilde{V}_2(\tilde{R},\tilde{r}) = \frac{V_2(R,r)}{V_0} = \left[\left(\frac{2}{3}-\frac{\beta_m^3}{3}+\beta_m\right)\pi R^3+\left(\frac{2}{3}-\frac{\beta_d^3}{3}+\beta_d\right)\pi r^3\right]\Big/\left(\frac{4}{3}\pi R_0^3\right)$$
$$= \left[\left(\frac{2}{3}-\frac{\beta_m^3}{3}+\beta_m\right)\left(\frac{R}{R_0}\right)^3+\left(\frac{2}{3}-\frac{\beta_d^3}{3}+\beta_d\right)\left(\frac{r}{R_0}\right)^3\right]\cdot\frac{3}{4}$$
$$= \tilde{R}^3\cdot\left[\left(\frac{1}{2}-\frac{\beta_m^3}{4}+\frac{3\beta_m}{4}\right)+\left(\frac{1}{2}-\frac{\beta_d^3}{4}+\frac{3\beta_d}{4}\right)\left(\frac{\tilde{r}}{\tilde{R}}\right)^3\right]$$

In summary,

$$\tilde{V}(\tilde{R},\tilde{r}) = \begin{cases}\tilde{V}_1(\tilde{R},\tilde{r}), \text{if before the critical state,}\\ \tilde{V}_2(\tilde{R},\tilde{r}), \text{if after the critical stat}\end{cases}$$

(2) After the geometrical quantities, we normalize the Lagrangian strain of any element from the mother,

$$\tilde{\epsilon}_m(\tilde{R}) = \frac{\epsilon_m(R)}{\epsilon_{m0}} = \frac{\frac{L_m(R)}{l_m}-1}{\frac{L_{m0}}{l_m}-1} = \frac{\frac{L_m(R)/R_0}{l_m/R_0}-1}{\frac{L_{m0}/R_0}{l_m/R_0}-1} = \frac{\tilde{L}_m(\tilde{R})/\tilde{l}_m-1}{\tilde{L}_{m0}/\tilde{l}_m-1}$$

and normalize the Lagrangian strain of any element from the daughter,

$$\tilde{\epsilon}_d(\tilde{r},\tilde{l}_d) = \frac{\epsilon_d(r,l_d)}{\epsilon_{m0}} = \frac{\frac{L_d(r)}{l_d}-1}{\frac{L_{m0}}{l_m}-1} = \frac{\frac{L_d(r)/R_0}{l_d/R_0}-1}{\frac{L_{m0}/R_0}{l_m/R_0}-1} = \frac{\tilde{L}_d(\tilde{r})/\tilde{l}_d-1}{\tilde{L}_{m0}/\tilde{l}_m-1}$$

(3) Lastly, we normalize the osmolyte concentration difference,

$$\tilde{C}(\tilde{N},\tilde{R},\tilde{r}) = \frac{C(N,R,r)}{C_0} = \frac{\frac{N}{V(R,r)}-c_{ex}}{\frac{N_0}{V_0}-c_{ex}} = \frac{\frac{N/N_0}{V(R,r)/V_0}-\frac{c_{ex}}{N_0/V_0}}{1-\frac{c_{ex}}{N_0/V_0}} = \frac{\frac{\tilde{N}}{\tilde{V}(\tilde{R},\tilde{r})}-\tilde{c}_{ex}}{1-\tilde{c}_{ex}}$$

(4) Finally, we plug all of these normalized quantities into the original Equations 8 and 23. We then obtain the normalized Newtonian equations for the mother (Equation 9) and for the daughter (Equation 10).

Reference values for normalization

Here are all the reference values that are used in all the normalized equations (referring to Table 1):

$$\begin{aligned}
S_{m0} &\equiv S_m(R_0) \equiv 2\pi R_0\left(R_0+\sqrt{R_0^2-\rho^2}\right)\\
V_0 &\equiv 4\pi R_0^3/3\\
C_0 &\equiv C(N_0,R_0,r_0) \equiv (N_0/V_0)-c_{ex}\\
\epsilon_{m0} &\equiv L_m(R_0)\Big/ l_m - 1 \equiv \frac{2R_0\cdot[\pi-\arcsin(\rho/R_0)]}{l_m}-1\\
a_{m0} &\equiv \pi\lambda C_0 R_0^2/M_m\\
\eta_0 &\equiv k_m h_{m0}\\
a_{d0} &\equiv \pi\lambda C_0 R_0^2/M_d
\end{aligned}$$

Implementation of the model

The whole budding process can be calculated/simulated through the following procedure (referring to Figure 2):

1. Initialization. Set the iteration step count $i = 0$, and each variable to its initial value $\tilde{N}_0$, $\tilde{R}_0$, $\tilde{r}_0$, $\tilde{\eta}_0$ and $0\tilde{l}_d$.
2. Set $\Delta\tilde{\eta}$ and $\Delta\tilde{N}$. In general, they can be different for each iteration step i, so we denote them generally as $(\Delta\tilde{\eta})_i$ and i$(\Delta\tilde{N})$.
3. "Weaken-fill" process: calculate $\tilde{R}_i'$ and $\tilde{r}_i'$ based on Equations 13 and 14.
4. "Repair" process: calculate $\tilde{l}_{di}''$ based on Equation 15, and calculate η_i'' based on Equation 18.
5. Update variable values. Set $\tilde{N}_{i+1} = \tilde{N}_i + (\Delta\tilde{N})_i$, $\tilde{R}_{i+1} = \tilde{R}_i'$, $\tilde{r}_{i+1} = \tilde{r}_i'$, $\tilde{\eta}_{i+1} = \tilde{\eta}_i''$ and $\tilde{l}_{d,i+1} = \tilde{l}_{di}''$. Set $1i = i+$.
6. Repeat from (ii).

With these procedures, we obtain the evolution of the cell's states along i, namely $(\tilde{N}_i,\tilde{R}_i,\tilde{r}_i,\tilde{\eta}_i,\tilde{l}_{di})$. Note that i is the iteration step count rather than real-time, so the evolution along i only represents successive changes of the cell (see STAR Methods - method details for more details).

The simulation procedure above means that if we know $(\Delta\tilde{\eta})_i$ and $(\Delta\tilde{N})_i$ at each iteration step i, we can completely calculate the whole budding process. Note that our formulas and simulation procedures are derived based on infinitesimal steps, so only the ratio $(\Delta\tilde{N})_i/(\Delta\tilde{\eta})_i$ (we denote this ratio as ψ_i) determines the solution, instead of their absolute values. We have the same argument when we use standard techniques to numerically solve differential equations: The time interval Δt in the differential equation should be set sufficiently small; and as long as Δt is sufficiently small (whatever the absolute value is), the numerical solution goes to the true solution. Above all, to completely simulate the budding process, we only need to know ψ_i. However, due to the following two reasons, in this paper, we focus only on the simplest case of assuming ψ_i to be a constant ψ. Firstly, while ψ is well-defined, we currently lack experimental data to provide a time series of ψ. In fact, experimentally measuring either $\Delta\tilde{N}/\Delta t$ or $\Delta\tilde{\eta}/\Delta t$ is not straightforward (these are used to calculate ψ, as per the definition in Equation 19). Secondly, the main motivation of this paper is to explore whether meaningful and logically consistent results (derived from the model) can be obtained in the simplest scenarios, thereby gaining insights into the mechanisms of budding. The empirical measurement of ψ is definitely worth further investigation in subsequent work, which will allow us to more specifically simulate and study the budding process.

Besides the key parameter ψ, there are three other parameters. The first is the radius of the chitin ring, $\tilde{\rho}$, which we set to 0.28, because most chitin rings cover 1% to 3% of the total surface area of the mother,[17,69] and we thus estimated $\tilde{\rho}$ by setting $\pi\tilde{\rho}^2/(4\pi\tilde{R}_0^2) = 0.2$. The second is the external osmolyte concentration, $\tilde{c}_{ex}$, which we set to 0.84, as seen from the data in[70] where the external and internal osmotic pressure in normal conditions is around 1.38 MPa and 1.65 MPa, respectively. Thirdly, we need to know the unstretched circumference of the mother, $\tilde{l}_m$, and the initial value of the unstretched circumference of the daughter, $\tilde{l}_{d0}$. Both of them can be calculated from $\tilde{V}_u$, the unstretched volume of the cell initially, namely the volume if the internal and the external osmolyte concentration are identical (which is also the so-called non-osmotic volume). For normal cells, $\tilde{V}_u$ was measured to be around 0.4.[23,70] Then, $\tilde{l}_m = 2(\pi - \arcsin\tilde{\rho})\sqrt[3]{\tilde{V}_u}$ and $\tilde{l}_{d0} = 2(\arcsin\tilde{\rho})\sqrt[3]{\tilde{V}_u}$. In addition, it is straightforward that other initial values are $\tilde{N}_0 = 1$, $\tilde{R}_0 = 1$, $\tilde{r}_0 = 1$ and $\tilde{\eta}_0 = 1$, because they are all normalized to their corresponding initial values.

Meaning of "iteration step" in the model

The iteration step, denoted as *i*, refers to the number of iterations used during the calculation of the entire budding process. The "iteration step" should be understood from a relative perspective. It is similar to solving differential equations, e.g., $df(t)/dt = c$. To solve it numerically, we need to write it in the form of a difference equation, $\Delta f(t) = c\cdot\Delta t$. By setting a value for Δt, one can integrate it to calculate $\Delta f(t)$ and consequently $f(t)$. The smaller the Δt, the more accurate the numerical solution for $f(t)$ will be, but it also requires more iterations. Generally speaking, as long as Δt is sufficiently small, the final solution will tend to be precise.

In this work, the "iteration step" *i* is analogous to the number of iterations used in the integration process for numerically solving differential equation $df(t)/dt = c$. Since, in this work, the process at each iteration is quasi-static, it allows us to solve for mechanical equilibrium at each iteration (referring to Figure 2 for the calculation of each iteration), using algebraic equations instead of differential equations. Similarly, to perform a numerical calculation, we need to set a value for Δt (the smaller Δt is, the more precise the calculated result will be, and a greater number of iteration steps will be needed). Therefore, the iteration step *i* should only be understood from a relative perspective.

We do not need a mechanism to determine the number of iterations required; in principle, one could continue calculating indefinitely (similar to differential equations, where *t*, or the iteration step *i*, can extend to infinity). Nevertheless, in this work, we choose to stop the calculation when the daughter cell's size significantly exceeds that of the mother, as it then loses biological relevance. Therefore, we can only interpret *i* relatively. In fact, the interval from $i = 0$ to the DETACH state can be considered as representing one cell cycle.

Daughter cell size variation

When $\psi = 0.15$, the daughter cell radius is 0.85 (as read from Figure 4E); thus, its volume is approximately $0.85^3 = 0.614$. When $\psi = 0.2$, the daughter cell radius is 0.95 (as read from Figure 4F); thus, its volume is approximately $0.95^3 = 0.857$. Therefore, the volume variation is $(0.857 - 0.614)/0.614 \approx 39.6\%$.

Abnormalities in wall integrity pathway

Here we examine if there are size changes in the newly-born daughters through budding in mutants with abnormalities in the cell wall integrity pathway. In our model, the key parameter ψ is not directly linked to the integrity pathway, so we cannot observe their response by merely altering ψ. However, we can modify Equation 18, which concerns the surface modulus of the daughter cell's wall. Equation 18 indicates that the daughter's cell wall can restore its strength (namely, surface modulus) after being stretched (following wall remodeling by enzymes, which is the "repair" process described by our model). Yet, if the mutant cell's wall integrity pathway is compromised, it would not return to its normal state. Here, we can "hack" into our model by forcibly altering the value of η' (Equation 18) to, for example, 95% or 85% of its original value, and then observe how the cell evolves thereafter. The results are shown in Figure S1.

From Figure S1A where the surface modulus η of the daughter cell wall only recovers to 95% compared to the previous time step, it can be observed that the maximum value of η during the entire cell cycle reaches about only 50% of the original (as indicated by the green line). This implies that regardless of when the daughter detaches from the mother, its cell wall strength will be significantly weakened. We can imagine that with each generation, the wall strength diminishes further, undoubtedly compromising normal cellular functions. The situation is even more severe when recovery is only 85%, as shown in Figure S1B.

The Abnormalities can be caused by many factors, e.g., Ace2-Δ[52,71] and Pkc1-Mpk1 pathway mutants.[72] The Pkc1-Mpk1 pathway regulates the synthesis of the cell wall, besides its roles in responding to cell wall stress and cell cycle regulation. Upon activation of Pkc1, a cascade of reactions ultimately activates Mpk1, which enters the nucleus to activate specific transcription factors. This, in turn, promotes the expression of genes related to cell wall synthesis, such as glucan synthases and chitin synthases. If the wall integrity mechanism is compromised (e.g., due to impairment of the Pkc1-Mpk1 pathway), experiments show that the size of daughter cells tends to decrease and their cell wall strength is weaker than normal, which is indeed consistent with the predictions of our model.[72]

As for Ace2, according to Talia et al. (2009), cells containing Ace2 have a larger "critical size" than cells lacking these factors. This may be the cumulative effect of numerous gene regulations.[52] On the other hand, Ace2 may also regulate processes in the later stages of budding; it is a transcription factor required for the destruction of the septum following cytokinesis. At the end of division, Ace2p specifically activates the transcription of genes such as CTS1, SCW11, DSE2, DSE3, and DSE4 in the daughter cell. These genes encode chitinases and glucanases, enzymes necessary for septum destruction and separation of mother and daughter cells post-budding. Ref. 71 shows that Ace2 Δ mutants result in increased cell size, because the absence of Ace2 prevents normal detachment of the daughter from the mother, leading to

continuous budding on the mother, hence increasing in size. In our model, this corresponds to the situation where, even after the mother shrinks back to its original size, the daughter does not detach and continues to grow, where we can see this from Figure 4.

Effects of osmotic pressure

Concerning the impact of osmotic pressure on cell division, there are few articles that discuss the effects of minor osmotic disturbances. Much research focuses on how cell division or the cell cycle changes under significant osmotic stress:

For instance, ref. 73 explores the dynamics and logic of yeast cells' response to osmotic shock by constructing a mathematical model. It was found that high osmotic pressure leads to the activation of a series of enzymes and gene expression, such as activating the HOG pathway to produce more glycerol to counterbalance the stress, ultimately achieving homeostasis. Experiments[74,75] also confirmed that under high osmotic pressure conditions, yeast cells activate the HOG pathway, adjusting gene expression and metabolism to adapt to this environment, which results in an elongated cell cycle. More specifically, ref. 76 indicates that if osmotic pressure is applied during the G1 phase, osmotic stress causes a temporary G1 arrest and the downregulation of cyclin expression, thereby delaying or temporarily blocking the transition from G1 to S phase.

Additionally, other works discuss extreme cases, such as ref. 77, which states that under very high osmotic stress, plasmolysis may occur, i.e., the cell membrane detaches from the cell wall, leading to growth stasis. Also, the study[78] applied oscillatory osmotic stress and combined glucose deprivation (which may frequently occur to cells in natural conditions). It was found that under this condition, cell division speeds up, survival time increases, and transcriptional response decreases. The higher the frequency of osmotic stress, the lower the rate of cell division.

However, under normal physiological conditions, discussions on the effects of minor osmotic changes are scarce; our model here aims to depict the budding process of yeast at normal physiological levels. Under such physiological conditions, the cell wall is quasi-static, meaning that the osmotic pressure is mechanically balanced with the tension provided by the cell wall (although this balance is occasionally disrupted, it is immediately restored). Therefore, even if the osmotic pressure changes, the cell state can be restored through self-regulation. As shown in Figure S2, where we simulated two scenarios: following the budding of the cell, we either increased or decreased the concentration of osmolytes in the extracellular environment, we can see the cell state undergoes a rapid change and then returns to normal. Ultimately, the changes in the state of the mother and daughter cells are minimal, indicating that cells can quickly return to homeostasis after experiencing minor osmotic disturbances. However, our model assumes that this homeostasis is achieved instantaneously—as depicted in the two figures above, where at $i = 2000$, there is a sudden response of the cell to return to homeostasis. In reality, this recovery is not instantaneous and would likely result in an extended cycle, a process not specifically captured in our model.

QUANTIFICATION AND STATISTICAL ANALYSIS

There are no quantification or statistical analyses to include in this study.